

Two-loop Quantum Corrections of Scalar QED with Non-minimal Chern-Simons Coupling

M.E. Carrington^{a,c}, W.F. Chen^{b,c}, G. Kunstatter^{b,c} and J. Mottershead^{b,d}

^a Department of Physics, Brandon University, Brandon, Manitoba, R7A 6A9 Canada

^b Department of Physics, University of Winnipeg, Winnipeg, Manitoba, R3B 2E9 Canada

^c Winnipeg Institute for Theoretical Physics, Winnipeg, Manitoba

^d Permanent Address: Physics Department, University of Alberta Edmonton, Alberta T6G 2J1, Canada

Abstract

We investigate two-loop quantum corrections to non-minimally coupled Maxwell-Chern-Simons theory. The non-minimal gauge interaction represents the magnetic moment interaction between the charged scalar and the electromagnetic field. We show that one-loop renormalizability of the theory found in previous work does not survive to two-loop level. However, with an appropriate choice of the non-minimal coupling constant, it is possible to renormalize the two-loop effective potential and hence render it potentially useful for a detailed analysis of spontaneous symmetry breaking induced by radiative corrections.

I. INTRODUCTION

Maxwell-Chern-Simons electrodynamics has been studied extensively in recent years for a variety of reasons. The Chern-Simons term gives the photon a topological mass without spontaneously breaking gauge symmetry [1] and allows for the existence of charged particles with fractional statistics [2]. Pure Chern-Simons scalar electrodynamics admits topological and non-topological self-dual solitons, for which many exact solutions to the classical equations of motion are available [3]. Moreover, such theories may also have physical significance. Relativistic three dimensional Chern-Simons theories provide a consistent description of the high temperature limit of four dimensional gauge theories [4], and certain solid state systems with planar dynamics [2]. In addition, the non-relativistic version of Maxwell-Chern-Simons theory has been applied to the fractional Hall effect, and more recently to rotating superfluid $^3\text{He-A}$ [5].

Recently a version of scalar electrodynamics in three dimensions has been studied in which a non-minimal Chern-Simons type gauge interaction was introduced. The non-minimal coupling in this model represents a magnetic moment interaction between the charged scalar and the electromagnetic field. It is of interest for several reasons. Firstly, it is well known that one of the most important features of scalar quantum electrodynamics (QED) is the occurrence of the Coleman-Weinberg mechanism [6]. In scalar QED with

non-minimal coupling, the Chern-Simons term is generated through the Coleman-Weinberg mechanism [7]. In this sense, the non-minimal model is the one in which the Chern-Simons term arises naturally rather than being put in by hand.

Another reason that the non-minimal model is of interest involves the study of vortex solutions. In recent years, the classical vortex solutions of 2+1-dimensional Chern-Simons field theories have received considerable attention [3, 8]. To find such a solution exactly, the model must be self-dual. A self-dual theory is one in which the classical equations of motion can be reduced from second- to first-order differential equations. In the absence of a Maxwell term, scalar QED with a Chern-Simons term is self-dual, and the topological and non-topological vortex solutions have been found with an appropriately chosen scalar potential [3]. However, if the Maxwell term is present, a self-dual Maxwell-Chern-Simons theory can be achieved only if a magnetic moment interaction between the scalar and the gauge field, i.e. the non-minimal Chern-Simons coupling, is introduced [8, 9].

It is well known that Maxwell-Chern-Simons scalar QED is renormalizable. Non-minimal gauge interactions are, however, notoriously non-renormalizable in four dimensions. There is some hope that the situation might be different in three dimensions. Some time ago it was found by two of us that the non-minimal Chern-Simons coupling in 2+1-dimensional scalar electrodynamics is actually renormalizable at the one-loop level [7]. The renormalizability occurs because the non-minimal gauge interaction contains the three-dimensional antisymmetric tensor. An analysis [7] of the symmetry breaking by induced radiative corrections shows that at the one-loop level the non-minimal model behaves differently from the minimally coupled one. In the usual Maxwell-Chern-Simons scalar QED, symmetry breaking results from quantum corrections but depends on the choice of a renormalization scale [10], whereas in the non-minimal model the symmetry breaking is unambiguous and there is a finite temperature phase transition to the symmetry restored state.

It is clearly of interest to discover whether the renormalizability of this model persists beyond one-loop level and to compare the symmetry breaking phase transitions in the minimal and non-minimal models at higher orders. The two-loop behaviour of the minimal model has recently been analyzed in detail [10] where it was shown that the Coleman-Weinberg mechanism occurs at two-loops. The purpose of the present paper is to commence a detailed analysis of the two-loop behaviour of the non-minimally coupled Maxwell-Chern-Simons theory. We will show that the model, not surprisingly, is not renormalizable at two-loop level. However, the two-loop effective potential can be made renormalizable providing certain conditions are satisfied by the coupling constants of the model. Thus we will show that under certain circumstances (i.e. when the lowest order in the momentum expansion is sufficient) the model may yield physically relevant predictions for the spontaneous symmetry breaking by radiative corrections at the two-loop level. A detailed analysis on the renormalized effective potential and the consequent symmetry breaking is deferred to a future publication.

The paper is organized as follows. Sect II is a brief review, containing an introduction to the model, a discussion of some technical aspects of dimensional regularization in 2+1 dimensions, and a list of some of the necessary Feynman rules. Sect III demonstrates that the full effective action is not renormalizable at the two loop-level. Sect IV is devoted to the (somewhat lengthy) calculation of the two-loop effective potential in the \overline{MS} subtraction scheme. In contrast to the one-loop case, the renormalizability of the two-loop effective potential requires a specific choice of the non-minimal coupling constant. Our conclusions

are summarized in Sect V, while some useful formulae are collected in the appendix.

II. SCALAR QED WITH NON-MINIMAL CHERN-SIMONS COUPLING

A. The Lagrangian

The Lagrangian for scalar QED in $2 + 1$ dimensions with a non-minimal Chern-Simons coupling is [7]

$$\mathcal{L} = \frac{1}{2}(D_\mu\phi)^*D^\mu\phi - \frac{1}{4}F_{\mu\nu}F^{\mu\nu} - \frac{i}{8}\gamma_0\epsilon^{\mu\nu\rho}F_{\nu\rho}[\phi^*D_\mu\phi - (D_\mu\phi)^*\phi] - \frac{\lambda}{6!}(\phi^*\phi)^3, \quad (1)$$

where the complex scalar field ϕ can be decomposed into the real and imaginary parts, $\phi = \chi + i\eta$; $F_{\mu\nu} = \partial_\mu A_\nu - \partial_\nu A_\mu$; $D_\mu\phi = \partial_\mu\phi + ieA_\mu\phi$, and γ_0 , e and λ are the non-minimal Chern-Simons coupling, the gauge coupling and the scalar self-interaction coupling constants, respectively. The dimensional assignments for the fields and coupling constants are as follows:

$$[A_\mu] = [\phi] = [e] = M^{1/2}, \quad [\gamma_0] = M^{-1/2}, \quad [\lambda] = M^0. \quad (2)$$

The negative mass dimension of γ_0 indicates that the theory is not renormalizable in general.

Following the standard technique to calculate the effective potential we first assume the existence of a non-vanishing vacuum expectation value for the scalar field $\langle\phi\rangle = v$ with v real, and shift the real part of the scalar field, $\chi \rightarrow \chi + v$ [11]. We look for a non-vanishing value of v by determining the minimum of the effective potential generated by quantum corrections. Note that in the Lagrangian (1), we have put the bare mass of the scalar field, the quartic scalar self-interaction coupling and the statistical parameter of a possible Chern-Simons term equal to zero, even though these terms are allowed by the gauge symmetry. The corresponding counterterms may appear, however, in the counterterm Lagrangian. The physical parameters can be obtained in the usual way, i.e. by choosing renormalization conditions that give zero renormalized parameters at $v = 0$. To avoid the infrared divergences we use the Landau-type R_ξ gauge [12]. The gauge-fixing term is

$$\mathcal{L}_{\text{g.f.}} = -\frac{1}{2\xi}(\partial_\mu A^\mu - \xi ev\eta)^2, \quad \xi = 0. \quad (3)$$

Up to a total derivative term, the Lagrangian can be divided into the kinetic part and ten interaction terms:

$$\begin{aligned} \mathcal{L}^{(0)} &= -\frac{1}{2}\chi\left(\partial^2 + \frac{\lambda}{4!}v^4\right)\chi - \frac{1}{2}\eta\left(\partial^2 + \frac{\lambda}{5!}v^4 - \xi e^2 v^2\right)\eta \\ &\quad + \frac{1}{2}A^\mu\left[(\partial^2 + e^2 v^2)g_{\mu\nu} - \left(1 - \frac{1}{\xi}\right)\partial_\mu\partial_\nu - \gamma_0 ev^2\epsilon_{\mu\nu\rho}\partial^\rho\right]A^\nu, \\ \mathcal{L}^{(1)} &= -\lambda\left(\frac{1}{6!}\chi^6 + \frac{1}{5 \times 4! \times 2!}\chi^4\eta^2 + \frac{1}{5 \times 4! \times 2!}\chi^2\eta^4 + \frac{1}{6!}\eta^6\right), \\ \mathcal{L}^{(2)} &= -\lambda v\left(\frac{1}{5!}\chi^5 + \frac{1}{5 \times 3! \times 2!}\chi^3\eta^2 + \frac{1}{5 \times 4!}\chi\eta^4\right), \end{aligned}$$

$$\begin{aligned}
\mathcal{L}^{(3)} &= -\lambda v^2 \left(\frac{1}{2 \times 4!} \chi^4 + \frac{1}{10 \times 2! \times 2!} \chi^2 \eta^2 + \frac{1}{10 \times 4!} \eta^4 \right), \\
\mathcal{L}^{(4)} &= -\frac{1}{3! \times 3!} \lambda v^3 \chi^3 - \frac{1}{5! \times 3! \times 2!} \lambda v^3 \chi \eta^2, \\
\mathcal{L}^{(5)} &= e A^\mu (\partial_\mu \eta \chi - \partial_\mu \chi \eta), \\
\mathcal{L}^{(6)} &= \frac{1}{2} \gamma_0 \epsilon^{\mu\nu\rho} \partial_\nu A_\rho (\chi \partial_\mu \eta - \eta \partial_\mu \chi), \\
\mathcal{L}^{(7)} &= \frac{1}{2} e^2 A_\mu A^\mu (\chi^2 + \eta^2), \\
\mathcal{L}^{(8)} &= -\frac{1}{2} \gamma_0 e \epsilon^{\mu\nu\rho} A_\mu \partial_\rho A_\nu (\chi^2 + \eta^2), \\
\mathcal{L}^{(9)} &= e^2 v A_\mu A^\mu \chi, \\
\mathcal{L}^{(10)} &= -\gamma_0 v e \epsilon^{\mu\nu\rho} A_\mu \partial_\rho A_\nu \chi.
\end{aligned} \tag{4}$$

B. Regularization

A regularization scheme must be chosen to handle the ultraviolet divergences of the theory. In this paper we shall use dimensional regularization. The use of dimensional regularization in a theory that explicitly depends on epsilon tensors involves adopting a complicated form for the gauge field propagator, as will be discussed below. In spite of this complication, dimensional regularization is simpler than the Pauli-Villars regularization adopted in the previous paper [7] since it allows us to preserve explicit gauge symmetry.

There are several problems involved with analytic continuation to n dimensions. The first of these is standard. The mass dimensions of the fields and parameters become,

$$[\phi] = [A_\mu] = [v] = M^{(n-2)/2}, \quad [e] = M^{(3-n)/2}, \quad [\gamma_0] = M^{(2-n)/2}, \quad [\lambda] = M^{2(3-n)}, \tag{5}$$

and thus, in order to ensure that the parameters keep their original mass dimensions, one must make the following replacements for the parameters in the regularized Lagrangian,

$$v \rightarrow \mu^{(n-3)/2} v, \quad e \rightarrow \mu^{(3-n)/2} e, \quad \gamma_0 \rightarrow \mu^{(3-n)/2} \gamma_0, \quad \lambda \rightarrow \mu^{2(3-n)} \lambda. \tag{6}$$

The second problem is more complicated. Dimensional regularization in a theory with a three-dimensional antisymmetric tensor $\epsilon_{\mu\nu\rho}$ must be handled carefully. It has been explicitly shown that naive dimensional regularization schemes cannot make the theory well defined when they are applied to a Chern-Simons type model [13]. Therefore, in carrying out dimensional regularization we must adopt the three-dimensional analogue of the consistent definition for γ_5 , which was originally proposed by 't Hooft and Veltman [14], and later given a strict mathematical justification by Breitenlohner and Maison [15]. The explicit definition of this dimensional continuation for Chern-Simons-type theory was explained in Ref. [16] where it is shown that this regularization method is indeed compatible with the Slavnov-Taylor identities. The explicit definition for the dimensional continuation of the epsilon and the metric tensors is

$$\begin{aligned}
\epsilon^{\mu\nu\rho} &= \begin{cases} \pm 1 & \text{if } (\mu\nu\rho) = \text{permutation of } (0, 1, 2) \\ 0 & \text{otherwise} \end{cases} \\
g_{\mu\nu} &= \begin{cases} +1 & \text{for } \mu = \nu = 0 \\ -1 & \text{for } \mu = \nu = 1, 2, \dots, n-1 \end{cases} \\
\tilde{g}_{\mu\nu} &= \begin{cases} +1 & \text{for } \mu = \nu = 0 \\ -1 & \text{for } \mu = \nu = 1, 2. \end{cases}
\end{aligned} \tag{7}$$

These definitions give rise to the following contractions,

$$\begin{aligned}
\epsilon^{\mu\nu\rho} \epsilon^{\lambda\eta}_{\rho} &= \tilde{g}^{\mu\lambda} \tilde{g}^{\nu\eta} - \tilde{g}^{\mu\eta} \tilde{g}^{\nu\lambda}, \quad g^{\mu\nu} \tilde{g}_{\nu}^{\lambda} = \tilde{g}^{\mu\lambda}, \\
\tilde{p}^{\mu} &= \tilde{g}^{\mu\nu} p_{\nu}, \quad \tilde{p}^2 = \tilde{p}_{\mu} p^{\mu}.
\end{aligned}$$

C. Feynman rules

The tree-level Feynman rules can be derived by standard functional integration techniques. The propagators for the scalar fields χ and η have the same form as in the four-dimensional case,

$$\begin{aligned}
iS_{\chi}(p) &= \frac{i}{p^2 - m_{\chi}^2}, \quad m_{\chi}^2 = \frac{\lambda}{4!} v^4; \\
iS_{\eta}(p) &= \frac{i}{p^2 - m_{\eta}^2}, \quad m_{\eta}^2 = \frac{\lambda}{5!} v^4.
\end{aligned} \tag{8}$$

Following Ref. [10] we can obtain the dimensional regularized propagator for the gauge field,

$$\begin{aligned}
iD_{\mu\nu}(p) &= i \left\{ - \left[\frac{(\gamma_0 ev^2)^2}{(p^2 - e^2 v^2)[(p^2 - e^2 v^2)^2 - p^2(\gamma_0 ev^2)^2]} + \frac{1}{p^2(p^2 - e^2 v^2)} \right] (\tilde{p}^2 \tilde{g}_{\mu\nu} - \tilde{p}_{\mu} \tilde{p}_{\nu}) \right. \\
&+ \frac{\gamma_0 ev^2}{(p^2 - e^2 v^2)^2 - p^2(\gamma_0 ev^2)^2} \epsilon_{\mu\nu\rho} i p^{\rho} - \frac{1}{p^2(p^2 - e^2 v^2)} [(p^2 g_{\mu\nu} - p_{\mu} p_{\nu}) - (\tilde{p}^2 \tilde{g}_{\mu\nu} - \tilde{p}_{\mu} \tilde{p}_{\nu})] \\
&+ \frac{(\gamma_0 ev^2)^3 (p^2 - \tilde{p}^2)}{[(p^2 - e^2 v^2)^2 - \tilde{p}^2(\gamma_0 ev^2)^2][(p^2 - e^2 v^2)^2 - p^2(\gamma_0 ev^2)^2]} \left[\frac{\gamma_0 ev^2}{p^2 - e^2 v^2} (\tilde{p}^2 \tilde{g}_{\mu\nu} - \tilde{p}_{\mu} \tilde{p}_{\nu}) \right. \\
&\left. \left. - \epsilon_{\mu\nu\rho} i p^{\rho} \right] \right\}.
\end{aligned} \tag{9}$$

The above expression can be rewritten as

$$\begin{aligned}
iD_{\mu\nu}(p) &= i \left\{ - \left[\frac{1}{m_1 + m_2} \left(\frac{1}{m_1} \frac{1}{p^2 - m_1^2} + \frac{1}{m_2} \frac{1}{p^2 - m_2^2} \right) - \frac{1}{m_3^2} \frac{1}{p^2} \right] (\tilde{p}^2 \tilde{g}_{\mu\nu} - \tilde{p}_{\mu} \tilde{p}_{\nu}) \right. \\
&+ \frac{1}{m_1 + m_2} \left(\frac{1}{p^2 - m_2^2} - \frac{1}{p^2 - m_1^2} \right) \epsilon_{\mu\nu\rho} i p^{\rho} \\
&\left. - \frac{1}{m_3^2} \left(\frac{1}{p^2 - m_3^2} - \frac{1}{p^2} \right) [(p^2 g_{\mu\nu} - p_{\mu} p_{\nu}) - (\tilde{p}^2 \tilde{g}_{\mu\nu} - \tilde{p}_{\mu} \tilde{p}_{\nu})] \right]
\end{aligned}$$

$$\begin{aligned}
& + \frac{(\gamma_0 ev^2)^3 (p^2 - \tilde{p}^2)}{[d^2 - \tilde{p}^2(\gamma_0 ev^2)^2][d^2 - p^2(\gamma_0 ev^2)^2]} \left[\frac{\gamma_0 ev^2}{p^2 - e^2 v^2} (\tilde{p}^2 \tilde{g}_{\mu\nu} - \tilde{p}_\mu \tilde{p}_\nu) - \epsilon_{\mu\nu\rho} i p^\rho \right] \Big\} \\
\equiv & -i \left\{ A(p) \left(\tilde{p}^2 \tilde{g}_{\mu\nu} - \tilde{p}_\mu \tilde{p}_\nu \right) - B(p) \epsilon_{\mu\nu\rho} i p^\rho + C(p) \left[(p^2 g_{\mu\nu} - p_\mu p_\nu) - (\tilde{p}^2 \tilde{g}_{\mu\nu} - \tilde{p}_\mu \tilde{p}_\nu) \right] \right. \\
& \left. + \frac{(\gamma_0 ev^2)^3 (p^2 - \tilde{p}^2)}{[d^2 - \tilde{p}^2(\gamma_0 ev^2)^2][d^2 - p^2(\gamma_0 ev^2)^2]} \left[\frac{\gamma_0 ev^2}{p^2 - e^2 v^2} (\tilde{p}^2 \tilde{g}_{\mu\nu} - \tilde{p}_\mu \tilde{p}_\nu) - \epsilon_{\mu\nu\rho} i p^\rho \right] \right\}, \quad (10)
\end{aligned}$$

where we have defined

$$\begin{aligned}
m_1 &= \frac{1}{2} ev \left(\sqrt{(\gamma_0 v)^2 + 4} + \gamma_0 v \right), \\
m_2 &= \frac{1}{2} ev \left(\sqrt{(\gamma_0 v)^2 + 4} - \gamma_0 v \right), \\
m_3^2 &= e^2 v^2, \quad d = p^2 - e^2 v^2,
\end{aligned} \quad (11)$$

and

$$\begin{aligned}
A(p) &= \frac{1}{m_1 + m_2} \left(\frac{1}{m_1} \frac{1}{p^2 - m_1^2} + \frac{1}{m_2} \frac{1}{p^2 - m_2^2} \right) - \frac{1}{m_3^2} \frac{1}{p^2}, \\
B(p) &= \frac{1}{m_1 + m_2} \left(\frac{1}{p^2 - m_1^2} - \frac{1}{p^2 - m_2^2} \right), \\
C(p) &= \frac{1}{m_3^2} \left(\frac{1}{p^2 - m_3^2} - \frac{1}{p^2} \right).
\end{aligned} \quad (12)$$

To further simplify the notation we make the following definitions,

$$S(p) = \frac{1}{p^2}, \quad S_i(p) = \frac{1}{p^2 - m_i^2}; \quad i = 1, 2, 3,$$

which allow us to write,

$$\begin{aligned}
A(p) &= \frac{1}{m_1 m_2 (m_1 + m_2)} [m_2 S_1 + m_1 S_2 - (m_1 + m_2) S], \\
B(p) &= \frac{1}{m_1 + m_2} [S_1 - S_2], \quad C(p) = \frac{1}{m_1 m_2} (S_3 - S).
\end{aligned} \quad (13)$$

These expressions obey the following identities:

$$\begin{aligned}
2e^2 v^2 (A - C) + e \gamma_0 v^2 B &= S_1 + S_2 + S_3, \\
e^2 v^2 (A - C) + e \gamma_0 v^2 B &= \frac{1}{m_1 + m_2} [m_1 S_1 + m_2 S_2 - (m_1 + m_2) S_3], \\
A - C &= \frac{1}{m_1 m_2 (m_1 + m_2)} [m_2 S_1 + m_1 S_2 - (m_1 + m_2) S_3], \\
e^2 A + \frac{1}{2} e \gamma_0 B &= \frac{1}{2 v^2} (S_1 + S_2 - 2S).
\end{aligned} \quad (14)$$

These expressions are useful to simplify calculations.

There are several mass poles in the dimensional regularized gauge field propagator. The first two terms in (10) show that m_1 and m_2 are the photon masses in the original three-dimensional space-time. The third term indicates that m_3 is the mass that photons acquire in $n - 3$ dimensional space-time. The last term is proportional to an evanescent quantity, $p^2 - \tilde{p}^2$, and the power-counting shows that this term behaves as $1/p^5$ for large p . In the two-loop calculation the contribution of this term at the level of regularization is finite and hence vanishes in the limit $n \rightarrow 3$.

The interaction vertices of the model were derived in Ref. [7]. These vertices are shown in Figs. 1-3 with dotted lines denoting gauge bosons, while solid lines corresponding to either the η field or the χ field, as labeled. For conciseness, the vertices in the figures are labeled purely by their number, so that for example $3b$ denotes V_{3b} , etc. The Feynman rules for the vertices and the corresponding interaction Lagrangians are as follows:

$$\begin{aligned}
\mathcal{L}^{(1)} &\rightarrow V_{1a}(\chi^6) = -i\lambda, \quad V_{1b}(\chi^4\eta^2) = V_{1b}(\chi^2\eta^4) = -i\lambda/5; \\
\mathcal{L}^{(2)} &\rightarrow V_{2a}(\chi^5) = -i\lambda v, \quad V_{2b}(\chi^3\eta^2) = V_{2c}(\chi\eta^4) = -i\lambda v/5; \\
\mathcal{L}^{(3)} &\rightarrow V_{3a}(\chi^4) = -i\lambda v^2/2, \quad V_{3b}(\chi^2\eta^2) = V_{3b}(\eta^4) = -i\lambda v^2/10; \\
\mathcal{L}^{(4)} &\rightarrow V_{4a}(\chi^3) = -i\lambda v^3/6, \quad V_{4b}(\chi\eta^2) = -i\lambda v^3/30; \\
\mathcal{L}^{(5)} + \mathcal{L}^{(6)} &\rightarrow V_5(\eta\chi A) + V_6(\eta\chi A) = e(p - q)_\lambda + i\gamma_0\epsilon^{\tau\alpha\lambda}k_\tau p_\alpha; \\
\mathcal{L}^{(7)} + \mathcal{L}^{(8)} &\rightarrow V_7(\chi^2 A^2) + V_8(\chi^2 A^2) = V_7(\eta^2 A^2) + V_8(\eta^2 A^2) = 2ie^2 g_{\alpha\beta} - e\gamma_0 v \epsilon_{\alpha\lambda\beta}(p - q)_\lambda; \\
\mathcal{L}^{(9)} + \mathcal{L}^{(10)} &\rightarrow V_9(\chi A^2) + V_{10}(\chi A^2) = -e\gamma_0 v \epsilon_{\mu\alpha\nu}(k - q)^\alpha + 2ie^2 v g_{\mu\nu}.
\end{aligned} \tag{15}$$

III. TWO-LOOP RENORMALIZABILITY

In this section we discuss the renormalizability of the theory at the two-loop level. In order to show that the theory is renormalizable we must show that contributions to the two-loop quantum effective action from terms that do not appear in the original Lagrangian are finite. The superficial degree of divergence (SDD) of a diagram is given by

$$\omega = 3L + \sum_v \delta_v v_v - 2I, \tag{16}$$

where L is the number of loops, I is the number of internal lines, δ_v is the number of derivatives associated with each vertex, and v_v is the number of vertices of each type. The sum is over all vertices in the diagram. We can rewrite this expression using the following relations,

$$\begin{aligned}
L &= I + 1 - V, \\
I &= \frac{1}{2} \sum_v i_v v_v, \\
l_v &= i_v + e_v,
\end{aligned} \tag{17}$$

where $V = \sum_v v_v$ is the number of vertices, l_v is the total number of lines entering vertex v , and i_v and e_v are respectively the number of internal and external lines entering the vertex v . Furthermore, there exists a relation between the number of vertices and lines,

$$\sum_v l_v v_v = 2I + E. \quad (18)$$

Using (17) with $L = 2$ this constraint can be written as

$$\sum_v (l_v - 2)v_v = 2 + E \quad (19)$$

Consequently, we have the SDD

$$\omega = 3 + \sum_v \omega_v v_v - \frac{1}{2}E, \quad (20)$$

where $\omega_v \equiv \delta_v + \frac{1}{2}l_v - 3$ is the degree of divergence for each vertex, which can be read out from the interaction Lagrangian (4),

$$\begin{aligned} \omega_1 &= 0, & \omega_2 &= -\frac{1}{2}, & \omega_3 &= -1, & \omega_4 &= -\frac{3}{2}, & \omega_5 &= -\frac{1}{2}, \\ \omega_6 &= \frac{1}{2}, & \omega_7 &= -1, & \omega_8 &= 0, & \omega_9 &= -\frac{1}{2}, & \omega_{10} &= -\frac{3}{2}. \end{aligned}$$

Substituting in we get,

$$\omega = 3 - \frac{1}{2}E + \left(-\frac{1}{2}v_2 - v_3 - \frac{3}{2}v_4 - \frac{1}{2}v_5 + \frac{1}{2}v_6 - v_7 - \frac{1}{2}v_9 - \frac{3}{2}v_{10} \right). \quad (21)$$

To explicitly verify the renormalizability, we need to look at the 1PI parts of the Green functions that have positive SDD but no correspondence in the classical Lagrangian. We consider the 1PI part of the four-point function of gauge fields, $A^4 \equiv \langle A_\mu A_\nu A_\lambda A_\rho \rangle$. It is straightforward to determine which combinations of vertices satisfy the two conditions (19) and (21). One must then select those combinations from which it is possible to obtain a diagram with four external photon lines. We categorize these diagrams in three groups: diagrams with two internal V'_6 's, one internal V_6 and no internal V_6 .

Note that when calculating the SDD of an A^4 diagram, the following points must be taken into account. If V_6 is an external vertex, then its degree of divergence is $\omega_6 = -1/2$ instead of $\omega_6 = 1/2$. This change occurs because of the fact that V_6 carries one factor of momentum from the photon line, which becomes an external momentum when V_6 is an external vertex. Similarly, the degree of divergence of V_8 is reduced to $\omega_8 = -1$ instead of $\omega_8 = 0$ when V_8 is an external vertex (V_8 is considered an external vertex if both photon lines are external legs). These exceptions must be considered in looking for divergent diagrams.

From (21) all diagrams with 2 V'_6 's have SDD = 2, 1, or 0. The diagrams with SDD equal to 0 and no external V'_8 's are shown in Figs. 4-10. It is straightforward to see that if the SDD is 2, then the graph has two external V'_8 's. As discussed above, these graphs have factors of the external photon momentum from the vertices V_8 which can be factored out, leaving a two-loop integral with SDD = 0. The diagrams are the same as those shown in Fig. 4, with the external V'_7 's replaced by V'_8 's. If the SDD is 1, then the diagram has one external V_8 . These graphs also have a factor of external photon momentum which can be factored out to leave an integral of SDD = 0. The diagrams are the same as those shown in Figs. 5-7 with the external V'_7 's replaced by V'_8 's.

The same thing happens for diagrams with one V_6 . The SDD is either 1 or 0. The diagrams with SDD equal to 0 and no external V'_8 s are shown in Figs. 11, 12. If the SDD is 1, then the diagram has an external V_8 which reduces the SDD to 0, with a prefactor that contains an external photon momentum. These diagrams are the same as those shown in Fig. 11 with the external V'_7 s replaced by V'_8 s. For the diagrams with no V_6 , all V'_8 s contribute one photon line which is internal and one which is external, and thus contribute the naive value $\omega_8 = 0$ to the counting of the diagram's SDD. All divergent diagrams have SDD=0 and are shown in Figs. 13-15.

Note that all of the diagrams with external V'_5 s have partner diagrams with all possible combinations and permutations of V'_5 s replaced by V'_6 s. These partner diagrams will have the same SDD=0 as the original diagrams, but they will contain additional factors of external photon momenta, since they contain external V'_6 s.

The above analysis shows that all the two-loop divergent diagrams for A^4 have SDD=0. For the purpose of studying renormalizability, we need to extract only the divergent parts and see whether they cancel. There are several simplifications that one can make when extracting the divergent part of a diagram with SDD=0. We start by considering the scalar propagator. When a scalar propagator (8) contains an external momentum it has the form

$$S(q+p, m) = \frac{1}{(q+p)^2 - m^2}$$

where p is an external momentum and q is an internal momentum that will be integrated over. To study the UV behaviour of this propagator we can employ following decomposition,

$$S(q+p, m) = \frac{1}{(q+p)^2 - m^2} = \frac{1}{q^2} - \frac{2p \cdot q + p^2 - m^2}{q^2 [(q+p)^2 - m^2]}. \quad (22)$$

The UV degree of divergence of the second term is one less than that of the first term and thus gives no contribution to the UV divergent part of the integral. Thus, in calculating the divergent part of the integral, we can make the replacement

$$S(q+p, m) \rightarrow S(q) \equiv 1/q^2. \quad (23)$$

To avoid the IR divergence induced by this procedure, it is necessary to keep the mass term at least in one propagator, i.e. replace $S(q+p, m)$ by $S(q, m)$. We will keep all three.

Similar simplifications are possible for the gauge propagator (10). Firstly, the evanescent parts of the gauge field propagator will give vanishing contribution to the UV divergent part of the integral in the limit $n \rightarrow 3$ since they have good UV behaviour. Secondly, the UV degree of divergence of the parity odd term in the gauge field propagator is one less than that of the parity even part of the propagator. Thus, there are no contributions to the UV divergent part of the integral from terms in the propagator that are proportional to the epsilon tensor. Lastly, as explained above for the scalar propagator, factors of external momentum can be dropped.

In addition, the calculation is simplified because of the fact that there are no UV divergences at one-loop in dimensional regularization. This fact is due to the special analytic properties of the one-loop amplitudes in odd dimensional space-time [17]. As a consequence, there is no need for us to consider the subtraction of sub-divergences.

Using the above observations, one can show that all divergent terms will be proportional to the two-loop integral of the form,

$$I = \int dk \int dq S(q) S(k) S(k+q, m) \quad (24)$$

with $dk \equiv d^3k/(2\pi)^3$. The divergence will appear as a pole of the form $1/(3-n)$.

We concentrate first on diagrams in which the prefactor does not depend on the external photon momentum (Figs. 4-15). These diagrams can be further classified into three groups by coupling constant prefactors. The first group of diagrams is shown in Figs. 4, 5, 8, 11, 13, 14 and is proportional to $e^2\gamma_0^2$, the second group is shown in Figs. 6, 7, 10, 12, 15 and is proportional to $e^4\gamma_0^2(\gamma_0 v)^2$. The third group are shown in Fig. 9 and is proportional to $e^4\gamma_0^2(\gamma_0 v)^4$. Each of these sets of diagrams must be separately finite if the theory is to be renormalizable. We will concentrate on the first group of diagrams, Figs. 4, 5, 8, 11, 13, 14. Direct calculation shows that the divergent pieces cancel between the diagrams in Figs. 4, 5, 8, 11, 13, while Fig. 14 is finite.

As a further check, we calculate the A^4 term with four external momentum factors. Gauge invariance requires that this contribution should take the form $(F_{\mu\nu})^4$, and renormalizability requires that it be finite. We obtain contributions from the diagrams in Fig. 8, with all of the external V'_5 's replaced by V'_6 's. Direct calculation shows that the divergent pieces cancel.

Unfortunately, further checking reveals that the action is not in fact renormalizable. We have calculated the χ^4 term with four external momentum factors. The corresponding diagrams are shown in Fig. 16. This term is a contribution to the gauge invariant structure $(D_\mu\phi)^4$ and must be finite if the action is to be renormalizable. We find that in this case the divergent terms do not cancel so that the two-loop quantum effective action is not renormalizable.

However, as we will show in the next section, the two-loop effective potential can be made renormalizable providing certain conditions are satisfied by the coupling constants in the model. Therefore, for the lowest order in the momentum expansion of the quantum effective action, the non-minimal model may yield physically relevant predictions for the spontaneous symmetry breaking by the radiative corrections at the two-loop level.

IV. THE EFFECTIVE POTENTIAL

The effective potential is the energy density of the vacuum in which the expectation value of the scalar field is given by $\langle\phi\rangle = v$ [11]. It can be determined from the effective action $\Gamma[\tilde{\phi}]$ according to

$$\Gamma[\tilde{\phi} = v] = -(2\pi)^n \delta^{(n)}(0) V_{\text{eff}}(v), \quad (25)$$

where $\tilde{\phi}$ is the vacuum expectation value of the scalar field in the presence of the external source. Using the fact that $\Gamma[\tilde{\phi}]$ is the generating functional of the proper vertex,

$$\Gamma[\tilde{\phi}] = \sum_{j=1}^{\infty} \frac{1}{j!} \int d^n x_1 d^n x_2 \cdots d^n x_j \Gamma^{(j)}(x_1, \dots, x_j),$$

one has

$$V_{\text{eff}}(v) = - \sum_{j=2}^{\infty} \frac{1}{j!} \Gamma^{(j)}(0, 0, \dots, 0) v^j, \quad (26)$$

which means that one can get the effective potential by calculating the 1PI vacuum diagrams. From Eq.(26) we can write [18]

$$V_{\text{eff}}(v) = V^{\text{tree}}(v) - \frac{i\hbar}{2} \int \frac{d^n p}{(2\pi)^n} \ln \det[iD^{-1}(p)] + i\hbar \left\langle \exp \left(\frac{i}{\hbar} d^n x \mathcal{L}_{\text{int}}(\hbar^{\frac{1}{2}} \phi, v) \right) \right\rangle_{\text{1PI}}, \quad (27)$$

where $D^{-1}(p)$ is the inverse propagator for each of the bosonic fields in the theory. V^{tree} is the tree potential and can be obtained directly from (1) as,

$$V^{\text{tree}} = \frac{\lambda}{6!} v^6 \quad (28)$$

The second term of (27) is the one-loop effective potential, and the third term contains the higher order contributions. We shall use this expression to get the two-loop contribution to the effective potential.

A. One-loop effective potential in dimensional regularization

The one-loop effective potential of this model was computed in Ref. [7] in Pauli-Villars regularization. In order to discuss spontaneous symmetry breaking, we now re-calculate the one-loop effective potential using dimensional regularization. According to (27) we have

$$V_{\text{eff}}^{\text{one-loop}} = \frac{\hbar}{2} \int \frac{d^n p}{i(2\pi)^n} \left\{ \ln[iS_{\chi}^{-1}(p)] + \ln[iS_{\eta}^{-1}(p)] + \ln \det[iD_{\mu\nu}^{-1}(p)] \right\}. \quad (29)$$

From the quadratic part $\mathcal{L}^{(0)}$ of the Lagrangian (4) we have the inverse scalar propagators

$$\begin{aligned} S_{\chi}^{(-1)}(p) &= p^2 - m_{\chi}^2, \\ S_{\eta}^{(-1)}(p) &= p^2 - m_{\eta}^2, \end{aligned}$$

and the inverse gauge field propagator

$$D_{\mu\nu}^{-1}(p) \equiv K_{\mu\nu} = (-p^2 + e^2 v^2) g_{\mu\nu} + \left(1 - \frac{1}{\xi}\right) p_{\mu} p_{\nu} - \gamma_0 e v^2 \epsilon_{\mu\nu\rho} i p^{\rho}, \quad (30)$$

which gives [10]

$$\det K_{\mu\nu} = \exp \text{Tr} \ln K_{\mu\nu} = \left(p^2 - e^2 v^2\right) \left(e^2 v^2 - \frac{1}{\xi} p^2\right) \left[(p^2 - e^2 v^2) - (\gamma_0 e v^2)^2 \tilde{p}^2\right]. \quad (31)$$

Substituting above results into Eq.(29) and making use of the integration formulas given in Ref. [10],

$$\begin{aligned} \int \frac{d^n p}{i(2\pi)^n} \ln(p^2 - m^2) &= -\frac{\Gamma\left(-\frac{1}{2}n\right)}{(4\pi)^{n/2}} m^n \stackrel{n \rightarrow 3}{=} -\frac{1}{6\pi} m^3; \\ \int \frac{d^n p}{i(2\pi)^n} \ln[(p^2 - e^2 v^2)^2 - (\gamma_0 e v^2)^2 \tilde{p}^2] &\stackrel{n \rightarrow 3}{=} -\frac{1}{6\pi} (ev)^3 (4 + \gamma_0^2 v^2)^{1/2} (1 + \gamma_0^2 v^2), \end{aligned} \quad (32)$$

we obtain the one-loop effective potential in the Landau gauge ($\xi = 0$),

$$\begin{aligned} V_{\text{eff}}^{\text{one-loop}} &= -\frac{\hbar}{12\pi} \left[m_\chi^3 + m_\eta^3 + (ev)^3 (4 + \gamma_0^2 v^2)^{1/2} (1 + \gamma_0^2 v^2) \right] \\ &= -\frac{\hbar}{12\pi} \left\{ \left[\left(\frac{1}{4!} \right)^{3/2} + \left(\frac{1}{5!} \right)^{3/2} \right] \lambda^{3/2} v^6 + (ev)^3 (4 + \gamma_0^2 v^2)^{1/2} (1 + \gamma_0^2 v^2) \right\}. \end{aligned} \quad (33)$$

This result agrees with the one obtained in [7]

B. Two-loop effective potential

It is straightforward to see that the two-loop effective potential is given by diagrams that contain only vertices from the cubic and quartic parts of the interaction Lagrangian. All of these diagrams are either ‘theta’ type diagrams, or ‘figure eight’ type diagrams. For each diagram we give the integral expression for the amplitude. The integral is evaluated by rotating to Euclidean space and using the integrals given in the appendix. The theta diagrams contain ultraviolet divergent terms and the results are separated into divergent and finite pieces. The divergent piece is represented by the integral I as defined in the appendix, and thus proportional to the factor

$$\frac{1}{3-n} - \gamma + 1 + \ln 4\pi$$

where γ is the Euler constant. As a last step we use (11) to write the results in terms of the fundamental parameters e , γ_0 and v .

(1). The ‘figure eight’ diagrams containing two scalar loops (Fig. 17)

These diagram are produced by the quartic interaction $\mathcal{L}^{(3)}$. The amplitude can be calculated by rotating to Euclidean space. We obtain,

$$\begin{aligned} V_{\text{eff}}^{(1)} &= -\hbar^2 \lambda v^2 \mu^{(3-n)} \int \frac{d^n q}{(2\pi)^n} \frac{d^n p}{(2\pi)^n} \left[\frac{3}{2} \frac{1}{(p^2 - m_\chi^2)(q^2 - m_\chi^2)} \right. \\ &\quad \left. + \frac{3}{10} \frac{1}{(p^2 - m_\eta^2)(q^2 - m_\eta^2)} + \frac{1}{10} \frac{1}{(p^2 - m_\chi^2)(q^2 - m_\eta^2)} \right] \\ &= \frac{\hbar^2 \lambda v^2}{16\pi^2} \left(\frac{3}{2} m_\chi^2 + \frac{3}{10} m_\eta^2 + \frac{1}{10} m_\chi m_\eta \right) \\ &= \frac{\hbar^2 \lambda^2 v^6}{16\pi^2} \left(\frac{3}{2} \frac{1}{4!} + \frac{3}{10} \frac{1}{5!} + \frac{1}{10} \frac{1}{\sqrt{5}} \frac{1}{4!} \right). \end{aligned} \quad (34)$$

(2). The ‘figure eight’ diagram containing one scalar loop and one gauge field loop (Fig. 18)

This diagram is produced by the quartic interactions $\mathcal{L}^{(7)}$ and $\mathcal{L}^{(8)}$. Its amplitude is

$$\begin{aligned}
V_{\text{eff}}^{(2)} &= i\hbar^2 \mu^{(3-n)} \int \frac{d^n p}{(2\pi)^n} \frac{d^n q}{(2\pi)^n} i D^{\mu\nu}(p) \left(2ie^2 g_{\mu\nu} - 2\gamma_0 e \epsilon_{\mu\nu\rho} \tilde{p}^\rho \right) \left(\frac{1}{q^2 - m_\chi^2} + \frac{1}{q^2 - m_\eta^2} \right) \\
&= 2e^2 \hbar^2 \mu^{(3-n)} \int \frac{d^n p}{(2\pi)^n} \frac{d^n q}{(2\pi)^n} \left\{ -2\tilde{p}^2 \left[\frac{1}{m_1 + m_2} \left(\frac{1}{m_1} \frac{1}{p^2 - m_1^2} + \frac{1}{m_2} \frac{1}{p^2 - m_2^2} \right) - \frac{1}{m_3^2} \frac{1}{p^2} \right] \right. \\
&\quad \left. - \frac{1}{m_3^2} \left(\frac{1}{p^2 - m_3^2} - \frac{1}{p^2} \right) [(n-1)p^2 - 2\tilde{p}^2] \right\} \left(\frac{1}{q^2 - m_\chi^2} + \frac{1}{q^2 - m_\eta^2} \right) \\
&\quad - 4\gamma_0 e \hbar^2 \mu^{(3-n)} \int \frac{d^n p}{(2\pi)^n} \frac{d^n q}{(2\pi)^n} \frac{\tilde{p}^2}{m_1 + m_2} \left(\frac{1}{p^2 - m_1^2} - \frac{1}{p^2 - m_2^2} \right) \left(\frac{1}{q^2 - m_\chi^2} + \frac{1}{q^2 - m_\eta^2} \right). \quad (35)
\end{aligned}$$

Rotating to Euclidean space we obtain

$$\begin{aligned}
V_{\text{eff}}^{(2)} &= -2e^2 \hbar^2 \mu^{(3-n)} \int \frac{d^n p}{(2\pi)^n} \frac{d^n q}{(2\pi)^n} \left[\frac{2}{m_1(m_1 + m_2)} \frac{\tilde{p}^2}{p^2 + m_1^2} + \frac{2}{m_2(m_1 + m_2)} \frac{\tilde{p}^2}{p^2 + m_2^2} \right. \\
&\quad \left. + \frac{n-1}{m_3^2} \frac{p^2}{p^2 + m_3^2} - \frac{2}{m_3^2} \frac{\tilde{p}^2}{p^2 + m_3^2} \right] \left(\frac{1}{q^2 + m_\chi^2} + \frac{1}{q^2 + m_\eta^2} \right) \\
&\quad - 4\gamma_0 e \hbar^2 \mu^{(3-n)} \int \frac{d^n p}{(2\pi)^n} \frac{d^n q}{(2\pi)^n} \frac{\tilde{p}^2}{m_1 + m_2} \left(\frac{1}{p^2 + m_1^2} - \frac{1}{p^2 + m_2^2} \right) \left(\frac{1}{q^2 + m_\chi^2} + \frac{1}{q^2 + m_\eta^2} \right) \\
&= \frac{\hbar^2}{4\pi^2} \frac{m_\chi + m_\eta}{m_1 + m_2} [e^2(m_1^2 + m_2^2) + \gamma_0 e(m_1^3 - m_2^3)] \\
&= \frac{\hbar^2}{4\pi^2} \frac{1}{v^2} \frac{m_\chi + m_\eta}{m_1 + m_2} (m_1^4 + m_2^4) = \frac{\hbar^2}{4\pi^2} \frac{1}{v^2} \frac{m_\chi + m_\eta}{m_1 + m_2} [(m_1^2 - m_2^2)^2 + 2m_1^2 m_2^2] \\
&= \frac{\hbar^2}{4\pi^2} \frac{\sqrt{\lambda/4!} + \sqrt{\lambda/5!}}{\sqrt{\gamma_0 v^2 + 4}} (ev)^3 [4(\gamma_0 v)^4 + (\gamma_0 v)^2 + 2]. \quad (36)
\end{aligned}$$

(3). The ‘theta’ diagrams constructed from scalar propagators (Fig. 19)

These diagrams come from the interaction $\mathcal{L}^{(4)}$ and contain UV divergences. Their contribution to the effective potential is

$$\begin{aligned}
V_{\text{eff}}^{(3)} &= -\frac{\hbar^2}{2} \frac{(\lambda v^3)^2 \mu^{(3-n)}}{3!^3} \int \frac{d^n p}{(2\pi)^n} \frac{d^n q}{(2\pi)^n} \frac{1}{(p^2 - m_\chi^2)(q^2 - m_\chi^2) [(p+q)^2 - m_\chi^2]} \\
&\quad - \frac{\hbar^2}{2} \frac{(\lambda v^3)^2 \mu^{(3-n)}}{(5! \times 3!)^2 \times 2!} \int \frac{d^n p}{(2\pi)^n} \frac{d^n q}{(2\pi)^n} \frac{1}{(p^2 - m_\eta^2)(q^2 - m_\eta^2) [(p+q)^2 - m_\chi^2]} \\
&= \frac{\hbar^2}{2} (\lambda v^3)^2 \left(\frac{1}{3!^3} + \frac{1}{(5 \times 3!)^2 \times 2!} \right) \frac{1}{32\pi^2} \left(\frac{1}{3-n} - \gamma + 1 + \ln 4\pi \right) \\
&\quad - \frac{\hbar^2}{2} (\lambda v^3)^2 \frac{1}{32\pi^2} \left[\frac{1}{3!^3} \ln \frac{9m_\chi^2}{\mu^2} + \frac{1}{(5 \times 3!)^2 \times 2!} \ln \frac{(2m_\eta + m_\chi)^2}{\mu^2} \right] \\
&\equiv V^{(3)\text{div}} + V^{(3)\text{finite}}. \quad (37)
\end{aligned}$$

(4). The ‘theta’ diagram composed of one gauge field propagator, one η propagator and one χ propagator (Fig. 20).

This diagram arise from the cubic interaction $\mathcal{L}^{(5)}$ and $\mathcal{L}^{(6)}$ and the UV divergence is present. Its contribution to the effective potential is

$$V_{\text{eff}}^{(4)} = \frac{i\hbar^2}{2} \mu^{(3-n)} \int \frac{d^n p}{(2\pi)^n} \frac{d^n q}{(2\pi)^n} \left\{ \left[e(p+2q)_\mu - i\gamma_0 \epsilon_{\mu\alpha\beta} q^\alpha p^\beta \right] \right. \\ \left. \times \left[e(p+2q)_\nu - i\gamma_0 \epsilon_{\nu\gamma\delta} p^\gamma q^\delta \right] iD^{\mu\nu}(p) iS_\eta(p+q) iS_\chi(q) \right\}. \quad (38)$$

Inserting the gauge field propagator (10), employing the identities (14) to simplify the expression and performing the following contractions,

$$(p+2q)_\mu (p+2q)_\nu \left(\tilde{p}^2 g_{\mu\nu} - \tilde{p}_\mu \tilde{p}_\nu \right) = 4 \left[\tilde{p}^2 \tilde{q}^2 - 4(\tilde{p} \cdot \tilde{q}) \right], \\ (p+2q)_\mu (p+2q)_\nu \left(p^2 g^{\mu\nu} - p^\mu p^\nu \right) = 4 \left[p^2 q^2 - (p \cdot q)^2 \right], \\ \left[(p+2q)_\mu \epsilon_{\nu\gamma\delta} p^\gamma q^\delta + \epsilon_{\mu\alpha\beta} q^\alpha p^\beta (p+2q)_\nu \right] \left(\tilde{p}^2 g_{\mu\nu} - \tilde{p}_\mu \tilde{p}_\nu \right) \\ = \left[(p+2q)_\mu \epsilon_{\nu\gamma\delta} p^\gamma q^\delta + \epsilon_{\mu\alpha\beta} q^\alpha p^\beta (p+2q)_\nu \right] \left(p^2 g^{\mu\nu} - p^\mu p^\nu \right) = 0, \\ \left[(p+2q)_\mu \epsilon_{\nu\gamma\delta} p^\gamma q^\delta + \epsilon_{\mu\alpha\beta} q^\alpha p^\beta (p+2q)_\nu \right] \epsilon^{\mu\nu\rho} p_\rho = 4 \left[\tilde{p}^2 \tilde{q}^2 - 4(\tilde{p} \cdot \tilde{q}) \right] \\ \epsilon_{\mu\alpha\beta} q^\alpha p^\beta \epsilon_{\nu\gamma\delta} p^\gamma q^\delta \left(\tilde{p}^2 g_{\mu\nu} - \tilde{p}_\mu \tilde{p}_\nu \right) = \tilde{p}^2 \left[(p \cdot q)^2 - \tilde{p}^2 \tilde{q}^2 \right], \\ \epsilon_{\mu\alpha\beta} q^\alpha p^\beta \epsilon_{\nu\gamma\delta} p^\gamma q^\delta \left(p^2 g^{\mu\nu} - p^\mu p^\nu \right) = p^2 \left[\tilde{p}^2 \tilde{q}^2 - 4(\tilde{p} \cdot \tilde{q}) \right], \\ \epsilon_{\mu\alpha\beta} q^\alpha p^\beta \epsilon_{\nu\gamma\delta} p^\gamma q^\delta \epsilon^{\mu\nu\rho} p_\rho = 0, \quad (39)$$

we obtain

$$V_{\text{eff}}^{(4)} = -\frac{\hbar^2}{2} \int \frac{d^n p}{(2\pi)^n} \frac{d^n q}{(2\pi)^n} \mu^{(3-n)} \left\{ \left[-\frac{1}{m_1(m_1+m_2)} S_1(p) - \frac{1}{m_2(m_1+m_2)} S_2(p) + \frac{1}{m_3^2} S(p) \right] \right. \\ \times S_\chi(q) S_\eta(p+q) \left(4e^2 + \gamma_0^2 \tilde{p}^2 \right) \left[\tilde{p}^2 \tilde{q}^2 - (\tilde{p} \cdot \tilde{q})^2 \right] \} \\ + \frac{\hbar^2}{2} \frac{4e\gamma_0}{m_1+m_2} \int \frac{d^n p}{(2\pi)^n} \frac{d^n q}{(2\pi)^n} \mu^{(3-n)} [S_1(p) - S_2(p)] S_\chi(q) S_\eta(p+q) \left[\tilde{p}^2 \tilde{q}^2 - (\tilde{p} \cdot \tilde{q})^2 \right] \\ - \frac{\hbar^2}{2} \frac{1}{m_3^2} \int \frac{d^n p}{(2\pi)^n} \frac{d^n q}{(2\pi)^n} \mu^{(3-n)} [S_3(p) - S(p)] S_\chi(q) S_\eta(p+q) \left\{ 4e^2 \left[p^2 q^2 - (p \cdot q)^2 \right] \right. \\ \left. - \left[4e^2 + \gamma_0^2 (p^2 - \tilde{p}^2) \right] \left[\tilde{p}^2 \tilde{q}^2 - (\tilde{p} \cdot \tilde{q})^2 \right] \right\}, \quad (40)$$

where the evanescent terms are thrown away since their contribution vanishes in the limit $n \rightarrow 3$. Using the integrals given in the appendix, we find for the divergent part,

$$V_{\text{eff}}^{(4)(\text{div})} = \frac{\hbar^2}{64\pi^2} \left(\frac{1}{3-n} - \gamma + 1 + \ln(4\pi) \right) \left(\left(\frac{4}{v^2} + \gamma_0^2 \right) \left(\frac{1}{2} ((m_1 - m_2)^2 + m_1 m_2) (m_\chi^2 + m_\eta^2) \right. \right. \\ \left. \left. - \frac{1}{4} (m_1^2 - m_2^2)^2 + \frac{1}{4} m_1 m_2 (m_1 - m_2)^2 - \frac{1}{4} m_1^2 m_2^2 \right) + \frac{1}{4} \gamma_0^2 (m_\chi^2 - m_\eta^2)^2 \right) \\ = -\frac{\hbar^2}{230400\pi^2} \left(\frac{1}{3-n} - \gamma + 1 + \ln(4\pi) \right) v^2 \left(-90e^2 \gamma_0^4 v^6 \lambda - 450e^2 \lambda v^4 \gamma_0^2 \right. \\ \left. + 900e^4 \gamma_0^6 v^6 + 6300e^4 v^4 \gamma_0^4 + 11700e^4 \gamma_0^2 v^2 - 360e^2 \lambda v^2 + 3600e^4 + \gamma_0^2 \lambda^2 v^6 \right), \quad (41)$$

and for the finite part,

$$\begin{aligned}
V_{\text{eff}}^{(4)(\text{finite})} = & -\frac{\hbar^2}{64\pi^2 v^2} (m_\chi^2 - m_\eta^2)^2 \ln \left(\frac{(m_\chi + m_\eta)^2}{\mu^2} \right) \\
& + \frac{\hbar^2(\gamma_0^2 v^2 + 4)m_2}{256\pi^2 v^2(m_1 + m_2)} ((m_\chi + m_\eta)^2 - m_2^2)((m_\chi - m_\eta)^2 - m_2^2) \ln \left(\frac{(m_\chi + m_2 + m_\eta)^2}{\mu^2} \right) \\
& + \frac{\hbar^2(\gamma_0^2 v^2 + 4)m_1}{256\pi^2 v^2(m_1 + m_2)} ((m_\chi + m_\eta)^2 - m_1^2)((m_\chi - m_\eta)^2 - m_1^2) \ln \left(\frac{(m_\chi + m_1 + m_\eta)^2}{\mu^2} \right) \\
& - \frac{\hbar^2(\gamma_0^2 v^2 + 4)}{1536\pi^2 v^2(m_1 + m_2)} (12(m_1^2 + m_2^2)(m_\chi^3 - m_\chi^2 m_\eta - m_\eta^2 m_\chi + m_\eta^3) + 5m_1^5 + 5m_2^5 \\
& - (m_1^3 + m_2^3)(10m_\chi^2 + 12m_\chi m_\eta + 10m_\eta^2) + m_3^2(m_1 + m_2)(10m_\chi^2 + 10m_\eta^2 - 5m_3^2) \\
& + 12(m_1^4 + m_2^4)(m_\chi + m_\eta)) \\
& - \frac{\hbar^2 \gamma_0^2}{7680\pi^2} (6m_1^4 + 6m_2^4 - (12m_\eta^2 + 12m_\chi^2 + 6m_3^2)(m_1^2 + m_2^2) + 25m_3^4 \\
& - 26(m_\chi^2 + m_\eta^2)m_3^2 + 60m_\eta m_\chi(m_\chi^2 + m_\eta^2) + 25(m_\chi^2 - m_\eta^2)^2) . \tag{42}
\end{aligned}$$

(5). The ‘theta’ diagram with one χ propagator and two gauge field propagators (Fig. 21).

The interaction Lagrangians yielding this diagram are $\mathcal{L}^{(9)}$ and $\mathcal{L}^{(10)}$. The corresponding contribution to the effective potential is,

$$\begin{aligned}
V_{\text{eff}}^{(5)} = & i\hbar^2 \int \frac{d^n p}{(2\pi)^n} \frac{d^n q}{(2\pi)^n} \mu^{(3-n)} \left\{ \left[2ie^2 v g_{\mu\lambda} + \gamma_0 v e \epsilon_{\mu\lambda\alpha} (\tilde{p}^\alpha - \tilde{q}^\alpha) \right] iD_{\lambda\rho}(q) \right. \\
& \left. \times iS_\chi(p+q) \left[2ie^2 v g_{\rho\nu} + \gamma_0 v e \epsilon_{\rho\nu\beta} (\tilde{p}^\beta - \tilde{q}^\beta) \right] iD_{\nu\mu}(p) \right\} . \tag{43}
\end{aligned}$$

Denoting

$$\begin{aligned}
V_{\mu\nu}(p, q) & \equiv 2ie^2 v g_{\mu\nu} + \gamma_0 v e \epsilon_{\mu\nu\rho} (\tilde{p}^\rho - \tilde{q}^\rho), \\
P_{\mu\nu}^{(T)} & \equiv p^2 g_{\mu\nu} - p_\mu p_\nu, \\
\tilde{P}_{\mu\nu}^{(T)} & \equiv \tilde{p}^2 \tilde{g}_{\mu\nu} - \tilde{p}_\mu \tilde{p}_\nu, \tag{44}
\end{aligned}$$

and performing the following contractions,

$$\begin{aligned}
V_{\mu\lambda}(p, q) V_{\rho\nu}(p, q) \tilde{P}^{(T)\mu\nu} \tilde{P}^{(T)\lambda\rho} = & -4e^4 v^2 \left[\tilde{p}^2 \tilde{q}^2 + (\tilde{p} \cdot \tilde{q})^2 \right] + (\gamma_0 v e)^2 \\
& \times \left[-(\tilde{p}^2 + \tilde{q}^2) \left(\tilde{p}^2 \tilde{q}^2 + (\tilde{p} \cdot \tilde{q})^2 \right) + 4\tilde{p}^2 \tilde{q}^2 (\tilde{p} \cdot \tilde{q}) \right], \\
V_{\mu\lambda}(p, q) V_{\rho\nu}(p, q) \tilde{P}^{(T)\mu\nu} P^{(T)\lambda\rho} = & -4e^4 v^2 \left[2\tilde{p}^2 q^2 - \tilde{p}^2 \tilde{q}^2 + (\tilde{p} \cdot \tilde{q})^2 \right] + (\gamma_0 v e)^2 \left[4\tilde{p}^2 q^2 (\tilde{p} \cdot \tilde{q}) \right. \\
& \left. - 2\tilde{p}^4 q^2 + \tilde{p}^4 \tilde{q}^2 - \tilde{p}^2 (\tilde{p} \cdot \tilde{q})^2 - q^2 (\tilde{p} \cdot \tilde{q})^2 - \tilde{p}^2 \tilde{q}^2 q^2 \right], \\
V_{\mu\lambda}(p, q) V_{\rho\nu}(p, q) P^{(T)\mu\nu} P^{(T)\lambda\rho} = & -4e^4 v^2 \left[(n-3)p^2 q^2 + p^2 q^2 + (p \cdot q)^2 \right] \\
& + (\gamma_0 v e)^2 \left[-2p^2 q^2 (\tilde{p}^2 + \tilde{q}^2) + 4p^2 q^2 (\tilde{p} \cdot \tilde{q}) \right. \\
& \left. - (p^2 + q^2)(\tilde{p} \cdot \tilde{q})^2 + (p^2 + q^2)\tilde{p}^2 \tilde{q}^2 \right],
\end{aligned}$$

$$\begin{aligned}
V_{\mu\lambda}(p, q)V_{\rho\nu}(p, q)\tilde{P}^{(T)\mu\nu}\epsilon^{\lambda\rho\gamma}iq_\gamma &= -2\gamma_0 v^2 e^3 \left[-4\tilde{p}^2 \tilde{p} \cdot \tilde{q} + 2(\tilde{p} \cdot \tilde{q})^2 + 2\tilde{p}^2 \tilde{q}^2 \right], \\
V_{\mu\lambda}(p, q)V_{\rho\nu}(p, q)P^{(T)\mu\nu}\epsilon^{\lambda\rho\gamma}iq_\gamma &= -4\gamma_0 v^2 e^3 \left[-2p^2 \tilde{p} \cdot \tilde{q} + 2p^2 \tilde{q}^2 + (\tilde{p} \cdot \tilde{q})^2 - \tilde{p}^2 \tilde{q}^2 \right], \\
V_{\mu\lambda}(p, q)V_{\rho\nu}(p, q)\epsilon^{\mu\nu\alpha}ip_\alpha\epsilon^{\lambda\rho\beta}iq_\beta &= 8e^4 v^2 \tilde{p} \cdot \tilde{q} + 2(\gamma_0 v e)^2 \left[(\tilde{p}^2 + \tilde{q}^2) \tilde{p} \cdot \tilde{q} \right. \\
&\quad \left. - \tilde{p}^2 \tilde{q}^2 - (\tilde{p} \cdot \tilde{q})^2 \right], \tag{45}
\end{aligned}$$

we get

$$\begin{aligned}
V_{\text{eff}}^{(5)} &= i\hbar^2 \int \frac{d^n p}{(2\pi)^n} \frac{d^n q}{(2\pi)^n} \mu^{3-n} e^2 v^2 S_\chi(p+q) \left\{ e^2 \left[-4e^2 C(p)C(q)p^2 q^2 (n-3) \right. \right. \\
&\quad - 16[A(p) - C(p)]C(q)\tilde{p}^2(q^2 - \tilde{q}^2) - 4C(p)C(q)[p^2 q^2 + (p \cdot q)^2] \\
&\quad - 4[A(p)A(q) - C(p)C(q)][\tilde{p}^2 \tilde{p}^2 + (\tilde{p} \cdot \tilde{q})^2] + 8B(p)B(q)\tilde{p} \cdot \tilde{q} \left. \right] \\
&\quad + e\gamma_0 \left[8A(p)B(q)[\tilde{p}^2 \tilde{q}^2 + (\tilde{p} \cdot \tilde{q})^2 - 2\tilde{p}^2 \tilde{p} \cdot \tilde{q}] + 16C(p)B(q)(p^2 - \tilde{p}^2)(\tilde{q}^2 - \tilde{p} \cdot \tilde{q}) \right] \\
&\quad + \gamma_0^2 \left[-4C(p)C(q)(p^2 - \tilde{p}^2)(q^2 - \tilde{q}^2)(\tilde{p}^2 - \tilde{p} \cdot \tilde{q}) - 4A(p)C(q)(q^2 - \tilde{q}^2)\tilde{p}^4 \right. \\
&\quad - C(p)A(q)(p^2 - \tilde{p}^2)(2\tilde{p}^2 \tilde{q}^2 + 2(\tilde{p} \cdot \tilde{q})^2 - 8\tilde{q}^2 \tilde{p} \cdot \tilde{q}) \\
&\quad + 2B(p)B(q)[(\tilde{p}^2 + \tilde{q}^2)\tilde{p} \cdot \tilde{q} - \tilde{p}^2 \tilde{q}^2 - (\tilde{p} \cdot \tilde{q})^2] \\
&\quad \left. \left. - 2A(p)A(q)[2\tilde{p}^2 \tilde{q}^2 (\tilde{p}^2 - (\tilde{p} \cdot \tilde{q})) - \tilde{p}^2 (\tilde{p}^2 \tilde{q}^2 - (\tilde{p} \cdot \tilde{q})^2)] \right] \right\}. \tag{46}
\end{aligned}$$

In deriving (46) we have used the fact that the integrand is invariant under the interchange $p \longleftrightarrow q$.

The calculation of this amplitude is quite lengthy. For clarity we divide the result in three parts. We label them V_{e^2} , $V_{e\gamma_0}$ and $V_{\gamma_0^2}$. They correspond to the terms proportional to e^2 , $e\gamma_0$ and γ_0^2 respectively in (46) above. In the expressions that appear below, the couplings e and γ_0 do not explicitly appear because we have used the relations (11) to write

$$\begin{aligned}
e^2 &= \frac{1}{v^2} m_3^2, \\
e\gamma_0 &= \frac{1}{v^2} (m_1 - m_2), \\
\gamma_0^2 &= \frac{1}{v^2} \frac{(m_1 - m_2)^2}{m_1 m_2}, \tag{47}
\end{aligned}$$

and eliminate the couplings in favour of the masses. This substitution allows us to combine all three terms to obtain the simplest expression possible for the final result of this diagram. As a last step we use (11) to write the result in terms of the fundamental parameters e , γ_0 and v . First, the e^2 part is

$$\begin{aligned}
V_{e^2} &= -\frac{3\hbar^2 \mu^{(2n-6)}}{16\pi^2 v^2} \left(\frac{1}{3-n} - \gamma + 1 + \ln(4\pi) \right) m_3^4 + \frac{\hbar^2 m_\chi^4}{32\pi^2 v_2} \ln \left(\frac{m_\chi^2}{\mu^2} \right) \\
&\quad - \frac{\hbar^2 m_1 (m_2^2 - m_\chi^2)^2}{16\pi^2 (m_1 + m_2) v^2} \ln \left(\frac{(m_2 + m_\chi)^2}{\mu^2} \right) - \frac{\hbar^2 m_2 (m_1^2 - m_\chi^2)^2}{16\pi^2 (m_1 + m_2) v^2} \ln \left(\frac{(m_1 + m_\chi)^2}{\mu^2} \right) \\
&\quad + \frac{\hbar^2 m_1^2 (4m_2^2 - m_\chi^2)^2}{32(m_1 + m_2)^2 \pi^2 v^2} \ln \left(\frac{(2m_2 + m_\chi)^2}{\mu^2} \right) + \frac{\hbar^2 m_2^2 (4m_1^2 - m_\chi^2)^2}{32(m_1 + m_2)^2 \pi^2 v^2} \ln \left(\frac{(2m_1 + m_\chi)^2}{\mu^2} \right)
\end{aligned}$$

$$\begin{aligned}
& + \frac{\hbar^2 m_3^2 ((m_1 - m_2)^2 - m_\chi^2)^2}{16(m_1 + m_2)^2 \pi^2 v^2} \ln \left(\frac{(m_1 + m_2 + m_\chi)^2}{\mu^2} \right) \\
& + \frac{\hbar^2 m_3^4 (-3(m_1 - m_2)^2 + 2m_\chi(m_1 + m_2 + m_\chi))}{8(m_1 + m_2)^2 \pi^2 v^2}; \tag{48}
\end{aligned}$$

The term proportional to $e\gamma_0$ is given by

$$\begin{aligned}
V_{e\gamma_0} = & - \frac{5\hbar^2 \mu^{(2n-6)}}{8\pi^2 v^2} \left(\frac{1}{3-n} - \gamma + 1 + \ln(4\pi) \right) (m_1 - m_2)^2 m_3^2 \\
& - \frac{\hbar^2 m_3^2 (m_1 - m_2)^2 (49m_1^2 + 49m_2^2 - 42(m_1 + m_2)m_\chi + 26m_3^2 - 12m_\chi^2)}{48(m_1 + m_2)^2 \pi^2 v^2} \\
& - \frac{\hbar^2 (4m_1^2 - m_\chi^2)^2 (m_2 - m_1)m_2}{16(m_1 + m_2)^2 \pi^2 v^2} \ln \left(\frac{(2m_1 + m_\chi)^2}{\mu^2} \right) \\
& + \frac{\hbar^2 (4m_2^2 - m_\chi^2)^2 (m_2 - m_1)m_1}{16(m_1 + m_2)^2 \pi^2 v^2} \ln \left(\frac{(2m_2 + m_\chi)^2}{\mu^2} \right) \\
& + \frac{\hbar^2 (m_1 - m_2)^2 ((m_1 - m_2)^2 - m_\chi^2)^2}{16(m_1 + m_2)^2 \pi^2 v^2} \ln \left(\frac{(m_1 + m_2 + m_\chi)^2}{\mu^2} \right) \\
& + \frac{\hbar^2 (m_1 - m_2)(m_2^2 - m_\chi^2)^2}{16\pi^2 (m_1 + m_2)^2 v^2} \ln \left(\frac{(m_2 + m_\chi)^2}{\mu^2} \right) \\
& - \frac{\hbar^2 (m_1 - m_2)(m_1^2 - m_\chi^2)^2}{16\pi^2 (m_1 + m_2)^2 v^2} \ln \left(\frac{(m_1 + m_\chi)^2}{\mu^2} \right); \tag{49}
\end{aligned}$$

The term proportional to γ_0^2 can be calculated in a similar way,

$$\begin{aligned}
V_{\gamma_0^2} = & - \frac{\hbar^2 (m_1 - m_2)^2}{64\pi^2 v^2} \left[\mu^{(2n-6)} \left(\frac{1}{3-n} - \gamma + 1 + \ln(4\pi) \right) (25(m_1^2 + m_2^2) - 35m_3^2 - 6m_\chi^2) \right. \\
& - \frac{2(4m_1^2 - m_\chi^2)^2}{(m_1 + m_2)^2} \ln \left(\frac{(2m_1 + m_\chi)^2}{\mu^2} \right) - \frac{2(4m_2^2 - m_\chi^2)^2}{(m_1 + m_2)^2} \ln \left(\frac{(2m_2 + m_\chi)^2}{\mu^2} \right) \\
& + \frac{(m_1^2 - m_\chi^2)^2 m_1}{(m_1 + m_2)m_3^2} \ln \left(\frac{(m_1 + m_\chi)^2}{\mu^2} \right) + \frac{(m_2^2 - m_\chi^2)^2 m_2}{(m_1 + m_2)m_3^2} \ln \left(\frac{(m_2 + m_\chi)^2}{\mu^2} \right) \\
& - \frac{(m_1 - m_2)^2 ((m_1 - m_2)^2 - m_\chi^2)^2}{(m_1 + m_2)^2 m_1 m_2} \ln \left(\frac{(m_1 + m_2 + m_\chi)^2}{\mu^2} \right) \\
& + \frac{1}{2310(m_1 + m_2)^2} \left(89981(m_1^4 + m_2^4) - 110880m_\chi(m_1^3 + m_2^3) \right. \\
& \left. - (3837m_3^2 + 28158m_\chi^2)(m_1^2 + m_2^2) + (-46200m_\chi m_3^2 + 9240m_\chi^3)(m_1 + m_2) \right. \\
& \left. - 19356m_\chi^2 m_3^2 + 34124m_3^4 \right]. \tag{50}
\end{aligned}$$

The final expression for $V_{\text{eff}}^{(5)}$ is obtained by combining (48), (49), and (50):

$$V_{\text{eff}}^{(5)} = V_{e^2} + V_{e\gamma_0} + V_{\gamma_0^2} \tag{51}$$

To summarize, in the \overline{MS} scheme, the effective potential to two loops is given by,

$$V_{\text{eff}} = V^{\text{tree}} + V_{\text{eff}}^{\text{one-loop}} + V_{\text{eff}}^{\text{two-loop}},$$

$$V_{\text{eff}}^{\text{two-loop}} \equiv V_{\text{eff}}^{(1)} + V_{\text{eff}}^{(2)} + V_{\text{eff}}^{(3)\text{finite}} + V_{\text{eff}}^{(4)\text{finite}} + V_{\text{eff}}^{(5)\text{finite}}. \quad (52)$$

Having obtained an expression for the effective potential, the next step is to absorb the divergent terms into renormalized coupling constants by choosing certain renormalization conditions. However, from (41), it is easy to see that $V_{\text{eff}}^{(4)\text{div}}$ contains terms proportional to v^8 . Since these terms would require counterterms that have no correspondence in the classical Lagrangian, we must require that they vanish to ensure the renormalizability of two-loop effective potential. This can be done by imposing the constraint,

$$\gamma_0^2(-90e^2\gamma_0^2\lambda + 900e^4\gamma_0^4 + \lambda^2) = 0 \quad (53)$$

The solutions to this equation are

$$\gamma_0^2 = 0 \quad \text{or} \quad \gamma_0^2 = \frac{(3 \pm \sqrt{5})\lambda}{60e^2}. \quad (54)$$

The first, trivial solution, merely verifies that the theory is renormalizable in the limit $\gamma_0 \rightarrow 0$. For the case of a finite non-minimal Chern-Simons coupling, we must choose one of the second solutions and impose a non-trivial relation between this non-minimal coupling and the other fundamental coupling constants of the theory. Note that our result that the non-minimal coupling depends on the fundamental couplings is consistent with the fact that in a theory without non-minimal Chern-Simons coupling the magnetic moment interaction would be generated through quantum corrections [19]. We should emphasize that Eq.[54] applies to the tree level couplings. Since it is not protected by any symmetry, it will probably be subject to quantum corrections. However, since we cannot go beyond two loops in this model, these corrections, which would affect the effective potential only at three loops, are not relevant.

V. SUMMARY AND CONCLUSIONS

We have studied in some details the two-loop quantum behaviour of $2 + 1$ -dimensional scalar QED with a non-minimal Chern-Simons coupling. As expected from dimensional arguments, the complete theory is not renormalizable beyond the one-loop level. This is not a major problem in principle, since the theory is most reasonably considered as an effective field theory describing magnetic moment interactions between the charged scalar and the electromagnetic fields. At this level the renormalizability is useful because it limits the number of parameters that must be introduced at each order in perturbation theory in order to make unambiguous predictions. We find that the effective potential, which is the zeroth order contribution to the quantum effective action in the momentum expansion, can be made renormalizable providing the fundamental couplings are related to the non-minimal one by the condition (54). It is of interest to further examine the effective potential with this condition imposed. The renormalization of the two-loop effective potential using a physical renormalization scheme is a straightforward but lengthy procedure. This, plus an analysis of the resulting symmetry breaking mechanism, will be the subject of a future publication.

Finally, we remark that the two-loop calculations presented above are extremely lengthy, in part due to the complicated form of the dimensionally regulated gauge field propagator. It would therefore be of interest to examine an alternative regularization scheme that preserves gauge invariance without the need to dimensionally continue the antisymmetric tensor. One excellent candidate is operator regularization, which was shown to greatly facilitate two-loop calculations in Chern-Simons theory [20].

ACKNOWLEDGMENTS

This work is supported by the Natural Sciences and Engineering Research Council of Canada. We are greatly indebted to R. Kobes for various useful discussions.

APPENDIX A: TWO-LOOP INTEGRATION FORMULAE

This appendix is a collection of the integration formulae used in the calculation of two-loop effective potential. Denoting $dk = d^n k / (2\pi)^n$ and using the following notation for the Euclidean space propagators:

$$\mathcal{S}_1(q) = \frac{1}{q^2 + m_1^2}, \quad \mathcal{S}_2(k) = \frac{1}{k^2 + m_2^2}, \quad \mathcal{S}_3(k+q) = \frac{1}{(k+q)^2 + m_3^2},$$

$$S^3 \equiv \mathcal{S}_1(q)\mathcal{S}_2(k)\mathcal{S}_3(k+q),$$

we introduce the following integrals:

$$I = \int dk dq S^3;$$

$$N_1 = \int dk \mathcal{S}(k), \quad N_2 = \int dk k^2 \mathcal{S}(k), \quad N_3 = \int dk k^4 \mathcal{S}(k);$$

$$K^{\mu\nu\lambda\tau} = \int dk dq q^\mu q^\nu k^\lambda k^\tau S^3; \quad T^{\mu\nu\lambda\tau} = \int dk dq q^\mu q^\nu q^\lambda k^\tau S^3;$$

$$L^{\mu\nu\alpha\beta\lambda\tau} = \int dk dq q^\mu q^\nu q^\alpha q^\beta k^\lambda k^\tau S^3; \quad R^{\mu\nu\alpha\beta\lambda\tau} = \int dk dq q^\mu q^\nu q^\alpha k^\beta k^\lambda k^\tau S^3.$$

Contracting the tensor indices in various combinations with the n - and three-dimensional metric tensors, we get the integrations needed for two-loop calculations,

$$K_1 = \int dk dq q^2 k^2 S^3, \quad K_2 = \int dk dq (k \cdot q)^2 S^3, \quad K'_1 = \int dk dq \tilde{q}^2 k^2 S^3$$

$$\tilde{K}_1 = \int dk dq \tilde{q}^2 \tilde{k}^2 S^3, \quad \tilde{K}_2 = \int dk dq (\tilde{k} \cdot \tilde{q})^2 S^3;$$

$$T_1 = \int dk dq q^2 (k \cdot q) S^3, \quad \tilde{T}_1 = \int dk dq \tilde{q}^2 (\tilde{k} \cdot \tilde{q}) S^3, \quad T_2 = \int dk dq q^2 (\tilde{k} \cdot \tilde{q}) S^3;$$

$$L_1 = \int dk dq q^4 k^2 S^3, \quad \tilde{L}_1 = \int dk dq \tilde{q}^4 \tilde{k}^2 S^3, \quad L_2 = \int dk dq q^2 (k \cdot q)^2 S^3,$$

$$\tilde{L}_2 = \int dk dq \tilde{q}^2 (\tilde{k} \cdot \tilde{q})^2 S^3, \quad L_3 = \int dk dq q^2 \tilde{q}^2 \tilde{k}^2 S^3, \quad L_4 = \int dk dq \tilde{q}^4 k^2 S^3,$$

$$L_5 = \int dk dq q^2 \tilde{q}^2 k^2 S^3, \quad L_6 = \int dk dq q^2 (\tilde{k} \cdot \tilde{q})^2 S^3;$$

$$\begin{aligned}
R_1 &= \int dk dq q^2 k^2 (q \cdot k) S^3, & R_2 &= \int dk dq (q \cdot k)^3 S^3, & R_3 &= \int dk dq \tilde{q}^2 \tilde{k}^2 (\tilde{k} \cdot \tilde{q}) S^3 \\
R_4 &= \int dk dq q^2 \tilde{k}^2 (\tilde{k} \cdot \tilde{q}) S^3, & R_5 &= \int dk dq q^2 k^2 (\tilde{k} \cdot \tilde{q}) S^3.
\end{aligned}$$

The results are listed below,

$$\begin{aligned}
I &= \frac{\mu^{2(n-3)}}{32\pi^2} \left[\frac{1}{3-n} - \gamma + 1 - \ln \frac{(m_1 + m_2 + m_3)^2}{4\pi\mu^2} \right]; \\
N_1 &= -\frac{\mu^{2(n-3)}}{4\pi} m, \quad N_2 = \frac{\mu^{2(n-3)}}{4\pi} m^3, \quad N_3 = -\frac{\mu^{2(n-3)}}{4\pi} m^5; \\
K_1 &= -\frac{\mu^{2(n-3)}}{16\pi^2} (m_1^3 + m_2^3) m_3 + m_1^2 m_2^2 I, \\
K_2 &= \frac{\mu^{2(n-3)}}{64\pi^2} \left[m_3^2 (m_1 m_3 + m_2 m_3 - m_1 m_2) - m_3 (3m_1^3 + 3m_2^3 + m_1^2 m_2 + m_2^2 m_1) \right. \\
&\quad \left. + (m_1^2 + m_2^2) m_1 m_2 \right] + \frac{1}{4} (m_1^2 + m_2^2 - m_3^2)^2 I, \\
K'_1 &= \frac{3}{n} K_1 \\
\tilde{K}_1 &= \frac{1}{n(n-1)(n+2)} [(9n+3)K_1 + (6n-18)K_2], \\
\tilde{K}_2 &= \frac{1}{n(n-1)(n+2)} [3(n-3)K_1 + 6(2n-1)K_2]; \\
T_1 &= \frac{\mu^{2(n-3)}}{32\pi^2} [m_1^3 (m_3 - m_2) + 2m_2^3 m_3 + m_1^2 m_2 m_3] - \frac{1}{2} m_1^2 (m_1^2 + m_2^2 - m_3^2) I, \\
\tilde{T}_1 &= \frac{15}{n(n+2)} T_1, \quad T_2 = \frac{3}{n} T_1; \\
L_1 &= \frac{1}{16\pi^2} \mu^{2(n-3)} \left[m_1^5 m_3 + m_2^3 m_3 (m_1^2 + m_2^2 + m_3^2) \right] - m_1^4 m_2^2 I, \\
L_2 &= \frac{1}{16\pi^2} \mu^{2(n-3)} \left\{ m_2 m_3 \left[\frac{1}{4} m_1^4 + m_2^4 + \frac{3}{4} m_1^2 m_2^2 - \frac{1}{4} m_1^2 m_3^2 + \frac{1}{3} m_2^2 m_3^2 \right] - \frac{1}{4} m_1^3 m_2 \left[m_1^2 + m_2^2 - m_3^2 \right] \right. \\
&\quad \left. + m_1 m_3 \left[\frac{1}{2} m_1^4 + \frac{1}{4} m_1^2 (m_1^2 + m_2^2 - m_3^2) \right] \right\} - \left[\frac{1}{4} m_1^6 + \frac{1}{2} m_1^4 (m_2^2 - m_3^2) + \frac{1}{4} m_1^2 (m_2^2 - m_3^2)^2 \right] I, \\
\tilde{L}_1 &= \frac{15}{n(n-1)(n+2)(n+8)} [(3n+13)L_1 + 8(n-3)L_2], \\
\tilde{L}_2 &= \frac{15}{n(n-1)(n+2)(n+8)} [(n-3)L_1 + 2(5n-4)L_2], \\
L_3 &= \frac{3}{n(n-1)(n+2)(n+8)} [(3n+2)(n+7)L_1 + 4(n+4)(n-3)L_2], \\
L_4 &= \frac{15}{n(n+2)} L_1, \quad L_5 = \frac{3}{n} L_1, \\
L_6 &= \frac{3}{n(n-1)(n+2)(n+8)} [(n+6)(n-3)L_1 + 2(3n^2 + 12n - 8)L_2]; \\
R_1 &= \frac{\mu^{2(n-3)}}{32\pi^2} [m_1^3 m_2^3 - m_3^3 (m_1^3 + m_2^3) - m_3 (m_1^5 + m_2^5)] + \frac{1}{2} (m_1^2 + m_2^2 - m_3^2) K_1,
\end{aligned}$$

$$\begin{aligned}
R_2 &= \frac{\mu^{2(n-3)}}{32\pi^2} \left[\frac{1}{3} (m_1^3 m_2^3 - m_3^3 (m_1^3 + m_2^3)) - m_3 (m_1^5 + m_2^5) \right] + \frac{1}{2} (m_1^2 + m_2^2 - m_3^2) K_2, \\
R_3 &= \frac{15}{n(n-1)(n+2)(n+4)} [R_1(5n-1) + 2R_2(n-3)], \\
R_4 &= \frac{15}{n(n+2)} R_1, \\
R_5 &= \frac{3}{n} R_1.
\end{aligned}$$

We have employed the following relations to facilitate the two-loop calculation,

$$\begin{aligned}
\tilde{K}_1 - \tilde{K}_2 &= \frac{6}{n(n-1)} (K_1 - K_2), \\
\tilde{L}_1 - \tilde{L}_2 &= \frac{30}{n(n-1)(n+2)} (L_1 - L_2), \\
L_3 - \tilde{L}_1 &= \frac{3(n-3)}{n(n-1)(n+2)(n+8)} [(3n+17)L_1 + 4(n-6)L_2], \\
L_4 - \tilde{L}_1 &= \frac{3(n-3)}{n(n-1)(n+2)(n+8)} [(n+7)L_1 - 8L_2], \\
L_5 - L_4 &= \frac{3(n-3)}{n(n+2)} L_1, \\
L_6 - \tilde{L}_2 &= \frac{3(n-3)}{n(n-1)(n+2)(n+8)} [(n+1)L_1 + 2(3n-4)L_2], \\
R_4 - R_3 &= \frac{15(n-3)}{n(n-1)(n+2)(n+4)} [(n+1)R_1 - 2R_2] \\
R_5 - R_4 &= \frac{3(n-3)}{n(n+2)} R_1.
\end{aligned}$$

REFERENCES

- [1] S. Deser, R. Jackiw and S. Templeton, Ann. Phys. (N.Y.) **140** (1982) 372; R. Jackiw and S. Templeton, Phys. Rev. **D23** (1983) 2291.
- [2] F. Wilczek (ed.), *Fractional Statistics, Superconductivity of Anyons* (World Scientific, Singapore, 1990); S. Forte, Rev. Mod. Phys. **64** (1992) 193.
- [3] J. Hong, Y. Kim and P.Y. Park, Phys. Rev. Lett. **64** (1990) 2230; R. Jackiw and E.J. Weinberg, Phys. Rev. Lett. **64** (1990) 2234; R. Jackiw, K. Lee and E. Weinberg, Phys. Rev. **D42** (1990) 3488.
- [4] D. Gross, R. Pisarski and L. Yaffe, Rev. Mod. Phys. **53** (1981) 43; R. Efraty and V.P. Nair, Phys. Rev. Lett. **68** (1992) 2891.
- [5] J. Goryo and K. Ishikawa, Phys. Lett **A** (1998) 246.
- [6] S. Coleman and E. Weinberg, Phys. Rev. **D7** (1973) 1888.
- [7] M.E. Carrington and G. Kunstatter, Phys. Rev. **D50** (1994) 2830.
- [8] A. Antilloón, J. Escalona and M. Torres, Phys. Rev. **D55** (1997) 6327.
- [9] M. Torres, Phys. Rev. **D46** (1992) R2295.
- [10] P.N. Tan, B. Tekin and Y. Hosotani, Phys. Lett. **B388** (1996) 611; Nucl. Phys. **B502** (1997) 483.
- [11] S. Coleman, *Aspects of Symmetry*, Chapter 5 (Cambridge University Press, 1985).
- [12] R. Pisarski and S. Rao, Phys. Rev. **D32** (1985) 2830.
- [13] M. Chaichian and W.F. Chen, Phys. Rev. **D58** (1998) 125004.
- [14] G. 't. Hooft and M. Veltman, Nucl. Phys. **B44** (1972) 189.
- [15] P. Breitenlohner and D. Maison, Comm. Math. Phys. **52** (1977) 11.
- [16] G. Giavarini, C.P. Martin and F. Ruiz Ruiz, Nucl. Phys. **B381** (1992) 222.
- [17] E.R. Speer, J. Math. Phys. **15** (1974) 1.
- [18] R. Jackiw, Phys. Rev. **D9** (1974) 1698.
- [19] I.I. Kogan, Phys. Lett. **B265** (1991) 83; I.I. Kogan and G.W. Semenoff, Nucl. Phys. **B368** (1992) 718; M. Chaichian, W.F. Chen and V.Ya. Fainberg, Eur. Phys. J. **C5** (1998) 545.
- [20] F.A. Dilkes and D.G.C. McKeon, Phys. Rev. **D52** (1995) 4668; D.G.C. McKeon and S.K.C. Wong, Int.J. Mod. Phys. **A10** (1995) 2181.

FIGURES

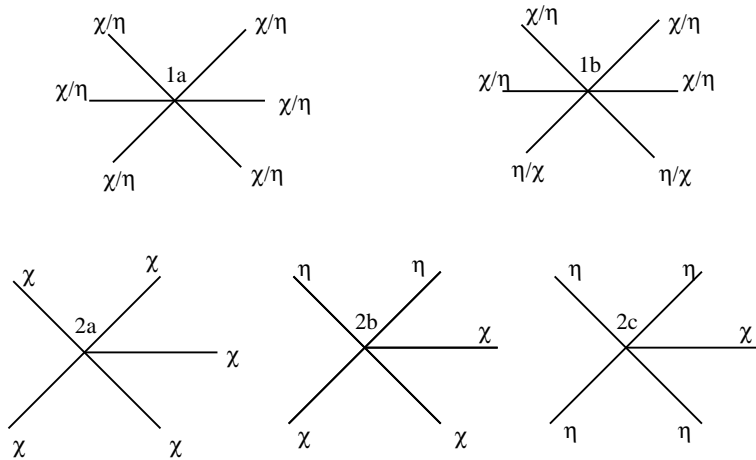


FIG. 1. Interaction vertices $V_{1a}, V_{1b}, V_{2a}, V_{2b}, V_{2c}$

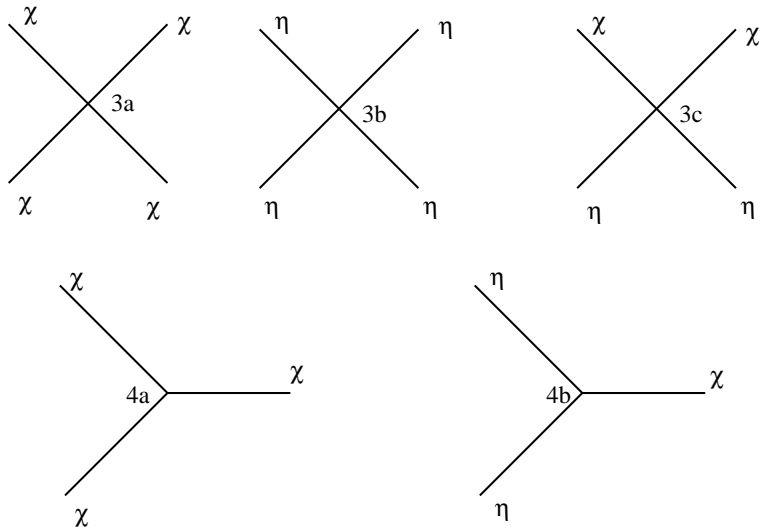


FIG. 2. Interaction vertices $V_{3a}, V_{3b}, V_{3c}, V_{4a}, V_{4b}$

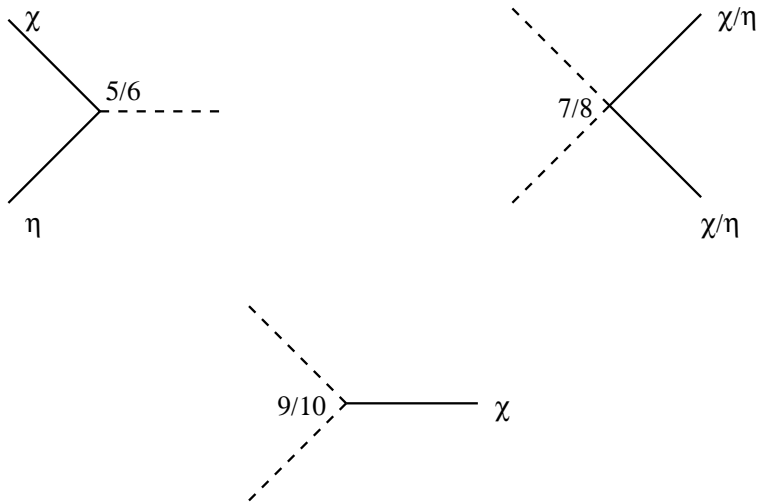


FIG. 3. Interaction vertices $V_5, V_6, V_7, V_8, V_9, V_{10}$

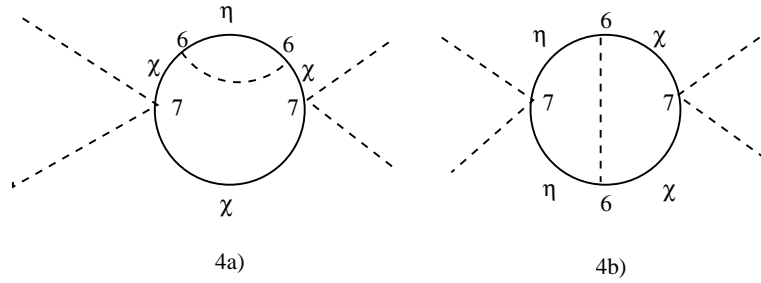


FIG. 4. Two loop contributions to A^4 part of the effective action.

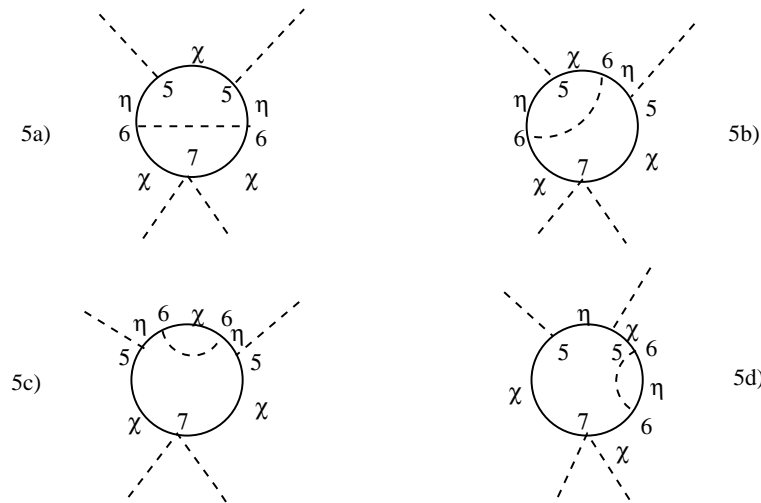


FIG. 5. Two loop contributions to A^4 part of the effective action.

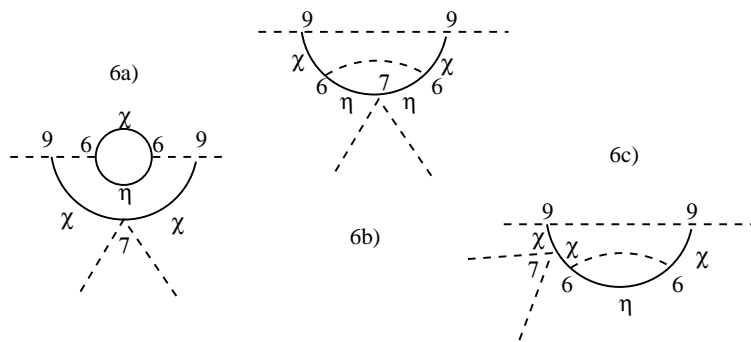


FIG. 6. Two loop contributions to A^4 part of the effective action.

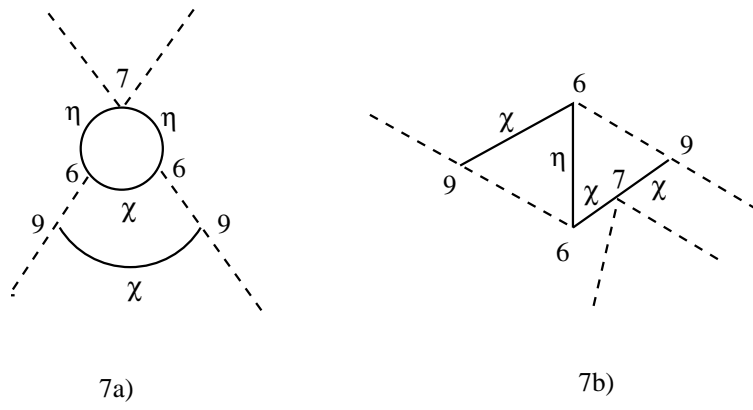


FIG. 7. Two loop contributions to A^4 part of the effective action.

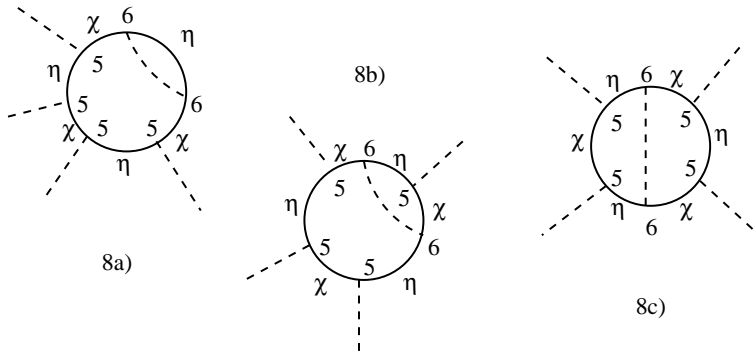


FIG. 8. Two loop contributions to A^4 part of the effective action.

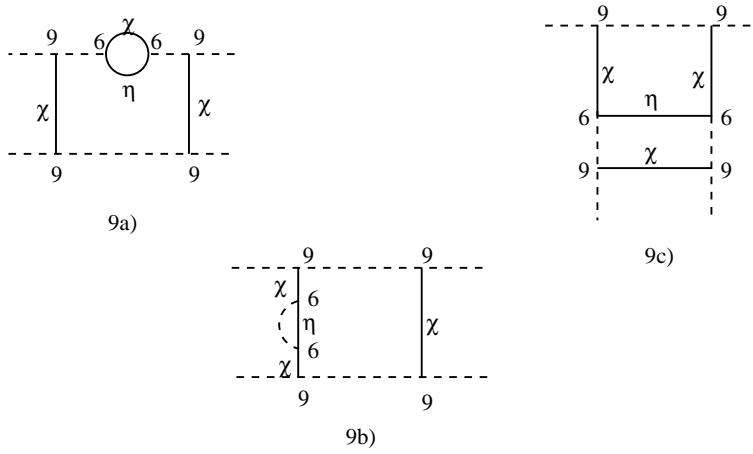


FIG. 9. Two loop contributions to A^4 part of the effective action.

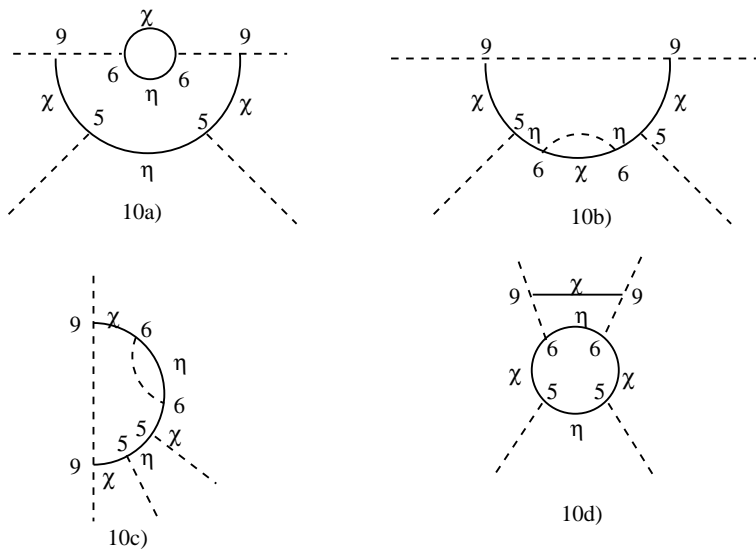


FIG. 10. Two loop contributions to A^4 part of the effective action.

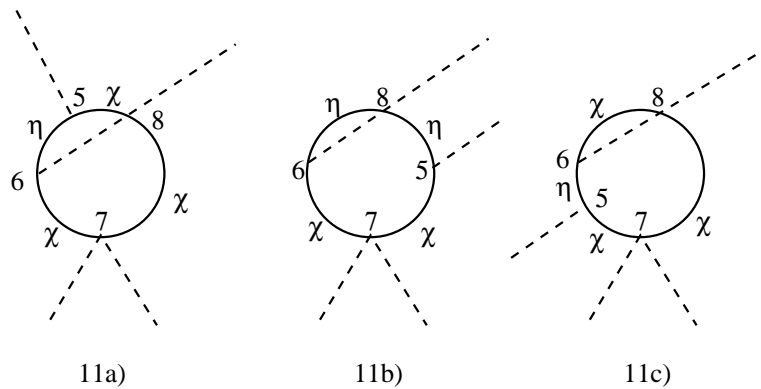


FIG. 11. Two loop contributions to A^4 part of the effective action.

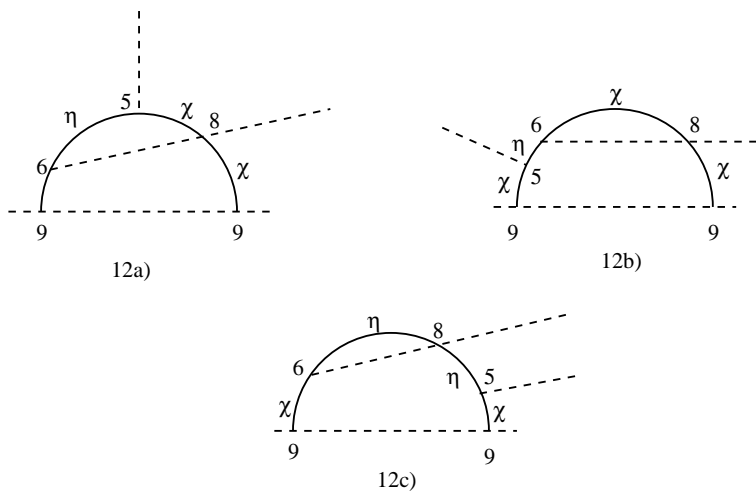


FIG. 12. Two loop contributions to A^4 part of the effective action.

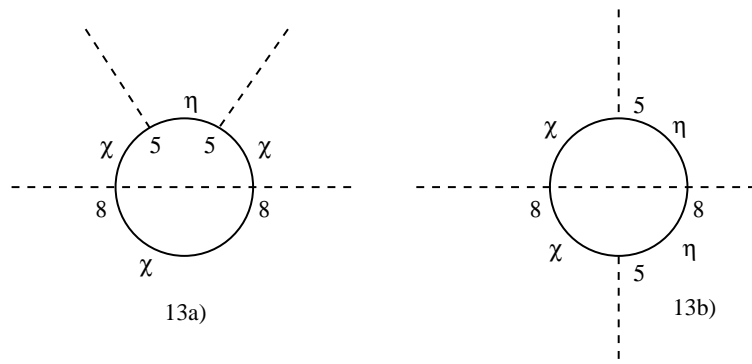


FIG. 13. Two loop contributions to A^4 part of the effective action.

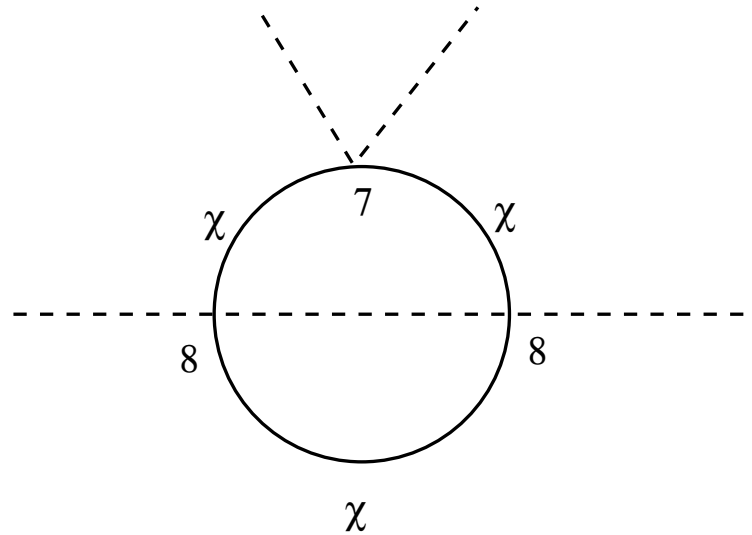


FIG. 14. Two loop contributions to A^4 part of the effective action.

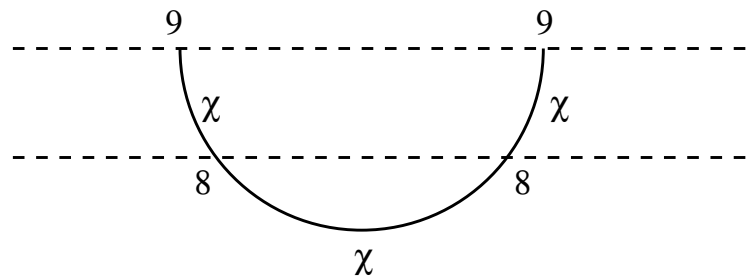


FIG. 15. Two loop contributions to A^4 part of the effective action.

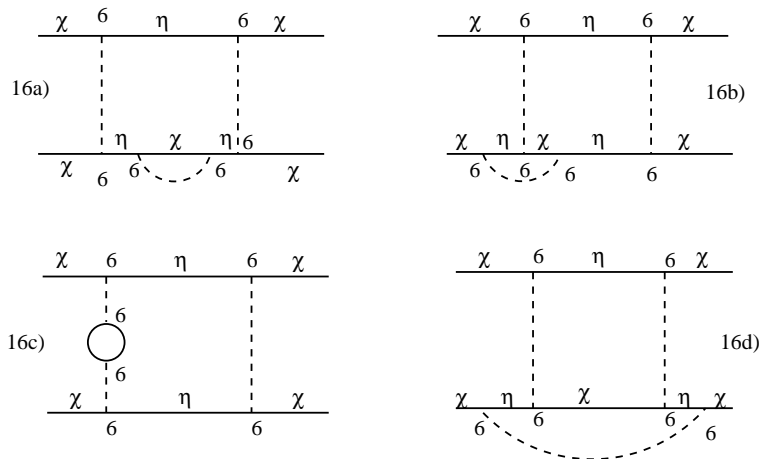


FIG. 16. Two loop contributions to A^4 part of the effective action.

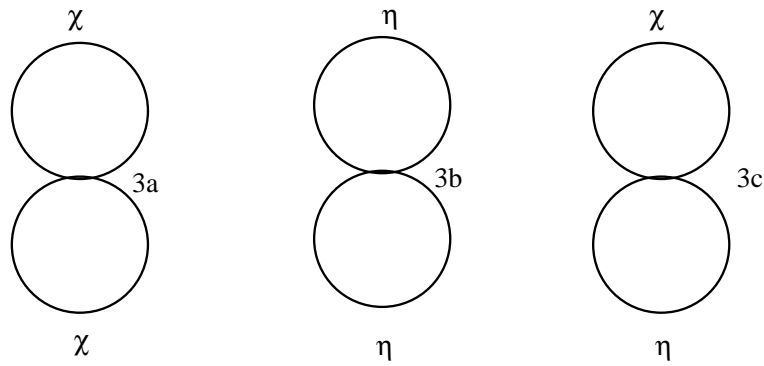


FIG. 17. Two loop contributions to the effective potential from two scalar loops.

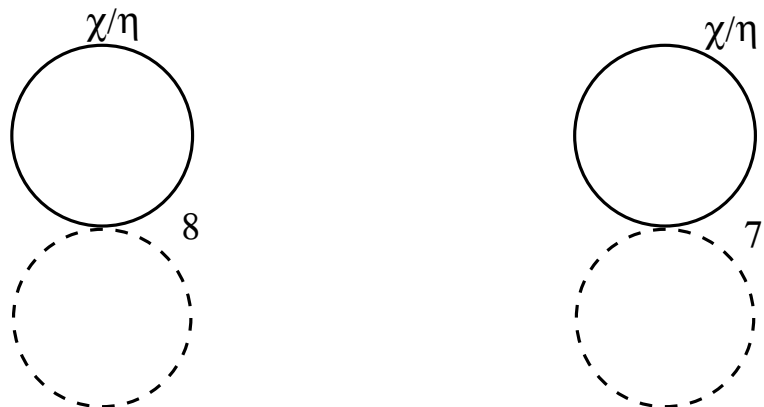


FIG. 18. Two loop contributions to the effective potential from one scalar and one gauge field loop.

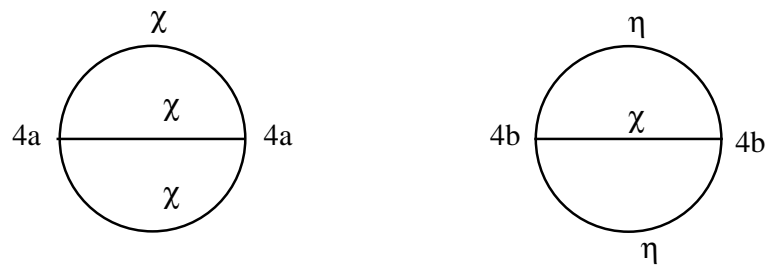


FIG. 19. Theta diagrams constructed from scalar propagators.

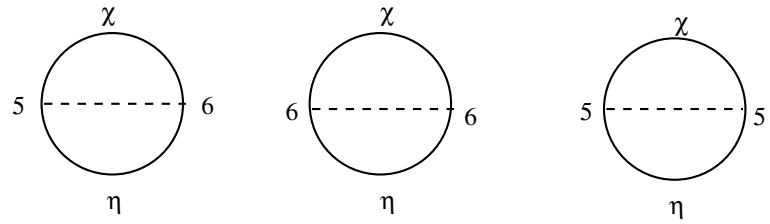


FIG. 20. Theta diagrams from one gauge field propagator and two scalar propagators

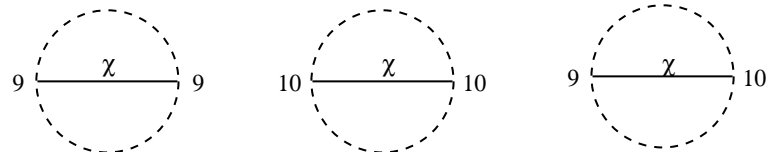


FIG. 21. Theta diagrams from two gauge field propagators and one scalar propagator.